Size Matters: The Influence of Isoform Size on the Intracellular Processing of Apolipoprotein(a)

by

Kristina Lu Han

A thesis submitted to the Department of Biochemistry

in conformity with the requirements for

the degree of Master of Science

Queen's University

Kingston, Ontario, Canada

(August, 2009)

Your file Votre référence
ISBN: 978-0-494-65179-7
Our file Notre référence
ISBN: 978-0-494-65179-7

Abstract

High plasma concentrations of Lipoprotein(a) (Lp(a)) have been identified as a risk factor for a variety of atherogenic disorders such as cerebrovascular disease, peripheral vascular disease, and coronary heart disease. Lp(a) consists of a lipoprotein moiety containing apolipoproteinB-100 (apoB-100), as well as apolipoprotein(a) (apo(a)), a unique glycoprotein to which the majority of Lp(a) functions are attributed. Variation in the number of identically repeated kringle IV type 2 (KIV_2) motifs of apo(a) forms the molecular basis of Lp(a) isoform size heterogeneity, which is a hallmark of this lipoprotein. There is a general inverse correlation between apo(a) size and plasma Lp(a) concentrations, attributed in part to less efficient secretion of larger apo(a) isoforms from hepatic cells. The present study provides a preliminary investigation into processes involved in apo(a) secretion, with respect to isoform size, to understand this inverse correlation at a molecular level. Pulse-chase experiments were performed in human embryonic kidney (HEK 293) cells and human hepatoma (HepG2) cells, both stably expressing differently-sized recombinant apo(a) isoforms representing the range of apo(a) sizes observed in the population. The folding kinetics for the different apo(a) isoforms were determined by changes in the mobility of the non-reduced radiolabelled species on SDS-PAGE gels. In HEK 293 cells, the rate at which apo(a) is folded correlated well with isoform size. In HepG2 cells, however, folding times were comparable regardless of isoform size. Apo(a) secretion from both cell lines exhibited size-dependency. Preliminary experimentation on endoplasmic reticulum (ER)-resident protein modifications of apo(a) was performed, resulting in the identification of apo(a) interactions with PDI, Erp57, Calnexin, Grp78, Grp94, and EDEM. Preliminary experiments indicate a role for intracellular apo(a) degradation in the amount of apo(a) that is secreted from HepG2 cells, although an isoform size dependency of this degradation process cannot be established with current experimental data. Further experimentation is required to confirm enzyme interactions

with differently-sized apo(a) isoforms, to identify other chaperones involved in apo(a) secretion, and to confirm the role of proteasomes in intracellular apo(a) degradation. This may, in turn, provide information regarding the mechanism of how apo(a) secretion from hepatic cells is regulated.

Acknowledgements

I would like to thank Dr. Marlys Koschinsky for giving me the wonderful opportunity to work on this project, and for her dedication and encouragement in difficult times. It has been a whirlwind of two years, and I have thoroughly enjoyed working under her supervision. I would also like to thank Dr. Michael Boffa for his advice and support on numerous aspects of this project. I would like to thank Dr. Graham Coté and Dr. Bruce Hill, who have provided me with valuable suggestions and experimental advice. This thesis project would not have been possible without the knowledge and support of fellow laboratory members Mathieu Garand and Nicole Feric. I would like to thank each member of the Koschinsky/Boffa laboratory, past and present for making my experience at Queen's University one filled with laughter, excitement, hilarity, and late-night discussions. I would like to thank Sue Johnston for being a terrific laboratory technician/mom to all of us. It has been an honour to work with everyone here at Queen's University.

Finally, I would like to thank my parents for their unconditional love and unwavering support, even when they thought their daughter was crazy for doing what she does.

Table of Contents

Abstract ii
Acknowledgements iv
Table of Contents v
List of Figures viii
List of Abbreviations ix
Chapter 1 Introduction 1
1.1 Lipoprotein(a) 1
1.2 Apolipoprotein(a) 1
1.3 Lp(a) Assembly 5
1.4 Lp(a) as a Risk Factor in Cardiovascular Diseases 7
1.4.1 Proatherogenic Properties of Lp(a) 7
1.4.2 Prothrombotic Properties of Lp(a) 9
1.5 The Contribution of Apo(a) Isoform Size to CHD Risk 12
1.6 Apo(a) Folding 13
1.7 ER-Resident Protein Interactions 15
1.7.1 Glucose-Regulated Protein 78/Binding Protein (Grp78/BiP) 16
1.7.2 Grp78 and the Unfolded Protein Response (UPR) 17
1.7.3 Glucose-Regulated Protein 94 (Grp94) 17
1.7.4 *N*-Linked Glycosylation and the Role of Calnexin and Calreticulin in the Process 18
1.7.5 ER-Associated Degradation (ERAD) 22
1.7.6 ER-Associated Degradation-Enhancing α-Mannosidase-like Protein (EDEM) 22
1.7.7 Protein Disulfide Isomerase (PDI) 23
1.7.8 ER Resident Protein 57 (Erp57/Grp58) 23
1.8 Apo(a) Intracellular Degradation 24
1.9 Rationale and Hypothesis 25
1.10 Specific Aims 27
Chapter 2 Materials and Methods 28
2.1 Materials 28
2.2 Cell Culture 29
2.3 Recombinant Apo(a) Isoform Construction and Expression 29
2.4 Apo(a) Folding Analysis 31

2.5 Apo(a) Immunoprecipitation....33
2.6 Apo(a) Secretion Kinetics in HepG2 cells....33
2.7 Apo(a)-ER Resident Protein Association Assay....33
2.8 Apo(a) Intracellular Degradation Inhibition Assay....34
2.9 SDS-Polyacrylamide Gel Electrophoresis (PAGE) and Immunoblotting....34
2.10 Apo(a) Folding Assay: Band Shift Distance Quantification....35
Chapter 3 Results....37
3.1 Analysis of Apolipoprotein(a) Folding....37
3.1.1 Apo(a) Folding in HEK 293 Cells....37
3.1.2 Apo(a) Folding in HepG2 Cells....38
3.2 Apolipoprotein(a) Secretion in HEK 293 Cells....41
3.3 Apolipoprotein(a) Secretion in HepG2 Cells....43
3.4 Apolipoprotein(a) Intracellular Modifications....45
3.4.1 Apo(a) interaction with PDI....45
3.4.2 Apo(a) interaction with Erp57....47
3.4.3 Apo(a) interaction with Calnexin....49
3.4.4 Apo(a) interaction with Grp78....49
3.4.5 Apo(a) interaction with Grp94....52
3.4.6 Apo(a) interaction with EDEM....52
3.5 Apolipoprotein(a) Intracellular Degradation....55
Chapter 4 Discussion....57
4.1 Analysis of Apolipoprotein(a) Folding....57
4.1.1 Analysis of Apo(a) Folding in HEK 293 Cell....59
4.1.2 Analysis of Apo(a) Folding in HepG2 Cells....60
4.2 Apolipoprotein(a) Secretion....63
4.3 Apolipoprotein(a) Intracellular Modifications....65
4.3.1 Apo(a) Interaction with PDI and Erp57....65
4.3.2 Apo(a) Association with Calnexin....66
4.3.3 Apo(a) Association with Grp78 and Grp94....67
4.3.4 Apo(a) Association with EDEM....68
4.3.5 Limitations of the Studies and Future Directions....69
4.4 Intracellular Degradation of Apolipoprotein(a)....70
Chapter 5 Conclusion....72

References 75

List of Figures

Figure 1: *Schematic representation of Lp(a)*. 2
Figure 2: *Relationship between apo(a) and plasminogen*. 3
Figure 3*: Two-step model for Lp(a) assembly*. 6
Figure 4*: Model for the inhibitory effect of apo(a) on fibrin-mediated plasminogen activation*... 11
Figure 5*: The N-linked glycan core*. 20
Figure 6*: The Calnexin/Calreticulin Cycle* 21
Figure 7***:** Recombinant-apo(a) constructs utilized in study* 30
Figure 8*: Schematic overview of the apo(a) folding assay*. 32
Figure 9*: Apo(a) folding patterns in HEK 293 Cells* 39
Figure 10: *Apo(a) folding patterns in HepG2 Cells*. 40
Figure 11*: Apo(a) secretion kinetics in HEK 293 cells*..... 42
Figure 12: *Apo(a) secretion kinetics in HepG2 cells* 44
Figure 13: *Intracellular association of apo(a) with Protein Disulfide Isomerase (PDI)*..... 46
Figure 14: *Intracellular association of apo(a) with ER Resident Protein 57 (Erp57)*..... 48
Figure 15: *Intracellular association of apo(a) with Calnexin*. 50
Figure 16: *Intracellular association of apo(a) with Glucose-Regulated Protein 78/Binding Protein (Grp78)* 51
Figure 17: *Intracellular association of apo(a) with Glucose-Regulated Protein 94 (Grp94)*…..53
Figure 18: *Intracellular association of apo(a) with ER Degradation-Enhancing α-Mannosidase-like (EDEM)* 54
Figure 19*: Inhibition of intracellular apo(a) degradation by the calpain inhibitor ALLN*..... 56

List of Abbreviations

ALLN	*N*-acetyl-leucyl-leucy-norleucinal
apo(a)	Apolipoprotein(a)
ApoB-100	Apolipoprotein B-100
CE	Cholesterol ester
CHD	Coronary heart disease
Cnx	Calnexin
Crt	Calreticulin
CST	Castanospermine
DMSO	Dimethyl sulfoxide
DSB	Dithiobis(succinimidyl propionate)
DTBP	Dimethyl 3,3`-dithiobispropionimidate
DTT	Dithiothreitol
EDEM	ER-associated degradation-enhancing α-mannosidase-like protein
ELISA	Enzyme-linked immunosorbent assay
ER	Endoplasmic Reticulum
ERAD	ER-associated degradation
ERGIC	ER-Golgi intermediate compartment
Erp57	ER resident protein 57
FBS	Fetal bovine serum
FC	Free cholesterol
Grp78/Bip	Glucose regulated protein 78/binding protein
Grp94	Glucose regulated protein 94
HEK 293	Human embryonic kidney 293 cell line

HepG2	Human hepatoma cell line
HRP	Horseradish peroxidase
HSP70	Heat shock protein 70
HSP90	Heat shock protein 90
IP	Immunoprecipitation
KDEL	Lys-asp-glu-leu sequence
LBS	Lysine binding site
LDL	Low-density lipoprotein
LMW	Low-molecular weight
Lp(a)	Lipoprotein (a)
M-apo(a)	Mature apolipoprotein(a)
McA-RH7777	Rat hepatoma McArdle RH7777 cell line
MEM	Minimal Essential Medium
NEM	*N*-ethylmalamide
PBS	Phosphate buffer saline
PDI	Protein Disulfide Isomerase
PL	Phospholipids
PMSF	phenylmethanesulphonylfluoride
PPI	Peptidyl prolyl isomerase
Pr-apo(a)	Precursor apolipoprotein(a)
R-apo(a)	Recombinant apolipoprotein(a)
SDS-PAGE	Sodium dodecyl sulfate-polyacrylamide gel electrophoresis
TG	Triglyceride
tPA	Tissue-type plasminogen activator

UDP	Uracil diphosophate
UGGT	UDP-glucose: glycoprotein glucosyltransferase
UMP	Uracil monophosphate
UPR	Unfolded protein response

Chapter 1
Introduction

1.1 Lipoprotein(a)

Lipoprotein(a) (Lp(a)) is a unique class of lipoproteins found in the plasma of humans and old world monkeys; a homologue has also been identified in the European hedgehog (1, 2). A schematic representation of the Lp(a) particle is shown in *Figure 1*. Lp(a) consists of a lipoprotein moiety containing apolipoproteinB-100 (apoB-100) that is indistinguishable from LDL in both lipid and apolipoprotein composition. The majority of unique Lp(a) functionalities are, however, attributed to its other component, a unique glycoprotein called apolipoprotein(a) (apo(a)) (3). Unlike other apolipoproteins, apo(a) is a hydrophilic, carbohydrate-rich glycoprotein that lacks amphipathic alpha helices (4).

1.2 Apolipoprotein(a)

McLean and colleagues reported striking similarities between apo(a) and the serine protease zymogen plasminogen based on the sequencing of a liver-derived apo(a) cDNA (5). The apo(a) gene, found on chromosome 6q27, evolved from the plasminogen gene during primate evolution by duplication, deletion, gene conversion, and mutation (6). The active form of plasminogen, plasmin, is a key enzyme involved in fibrinolysis (4). Apo(a) contains a number of repeated copies of sequences similar to plasminogen kringle IV (KIV), followed by sequences homologous to the plasminogen kringle V(KV) and serine protease (P) domains (*Figure 2*). Apo(a) isoforms are named using the number of KIV motifs present, followed by the letter K. Kringle domains are tri-looped protein structural motifs, characterized by three invariant disulfide bonds, and are found in a number of proteins in the thrombotic and fibrinolytic pathways (5).

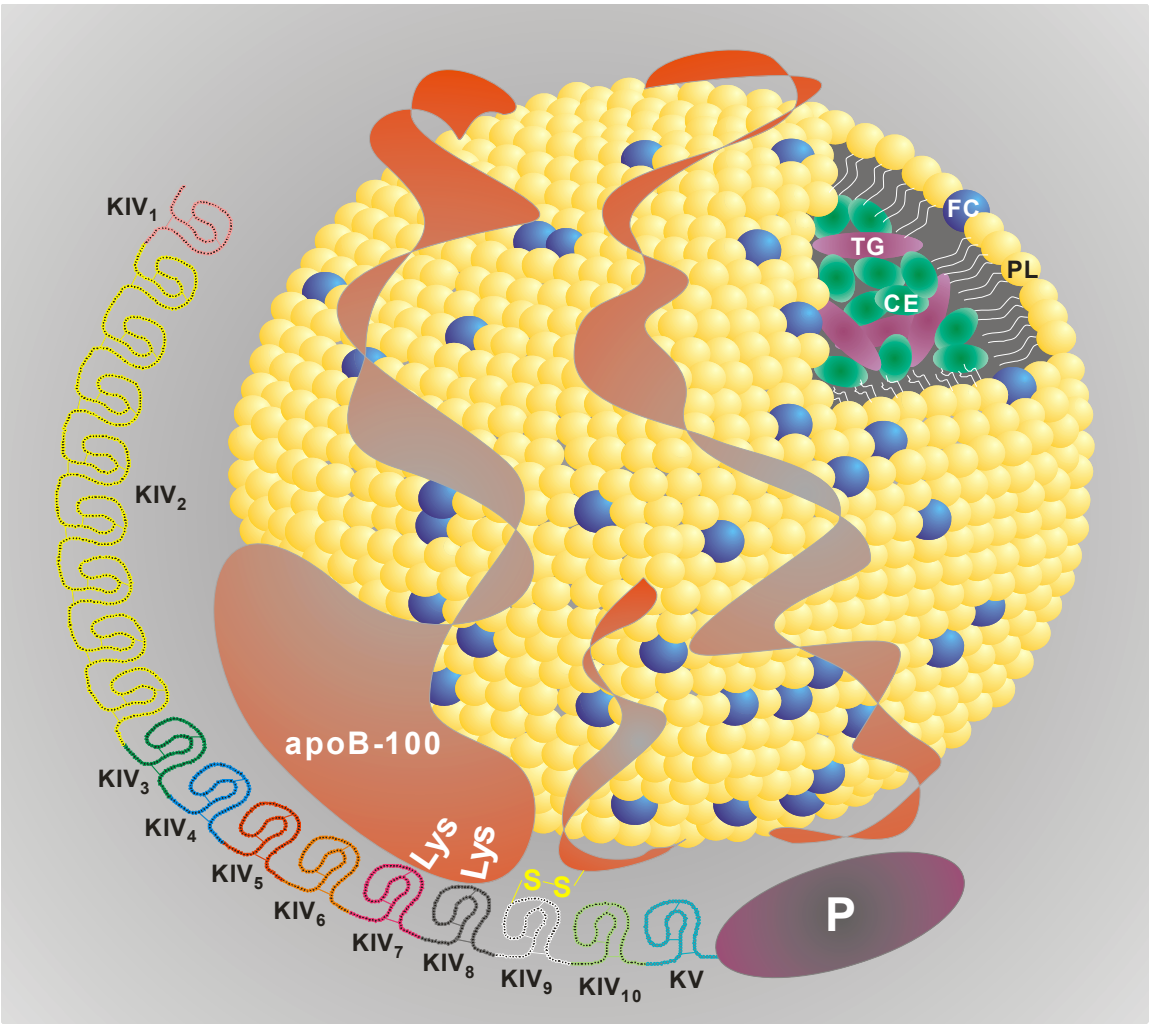

Figure 1: *Schematic representation of Lp(a):* Lp(a) constitutes a unique class of lipoprotein particles found in the plasma of humans and old world monkeys. It is very similar to low-density lipoprotein (LDL); both contain a cholesterol ester (CE) and triglyceride (TG) core surrounded by a monolayer of phospholipids (PL) and free cholesterol (FC), as well as a molecule of apolipoproteinB-100 (apoB-100). Lp(a) is distinguishable from LDL in that it contains an additional large glycoprotein, apolipoprotein(a) [apo(a)], that is covalently linked via a single disulfide bond to apoB-100. Apo(a) contains 10 types of KIV domains (designated KIV_{1-10}), which are distinguishable from each other by small variations in amino acid sequence (5, 7). Each KIV motif is present in a single copy except for KIV_2, which is present in 3 to >30 identically repeated copies attributable to allelic variations in the number of sequences encoding KIV in the apo(a) gene (8). This forms the basis of the Lp(a) size heterogeneity evident in the human population (9). Type 7 (pink) and type 8 (grey) kringle domains possess weak lysine binding sites (LBS) essential in the non-covalent step of Lp(a) assembly, while KIV_9 (white) contains an unpaired cysteine residue that is required for the covalent bond formation between apo(a) and apoB-100, (10, 11). Modified from Koschinsky (4).

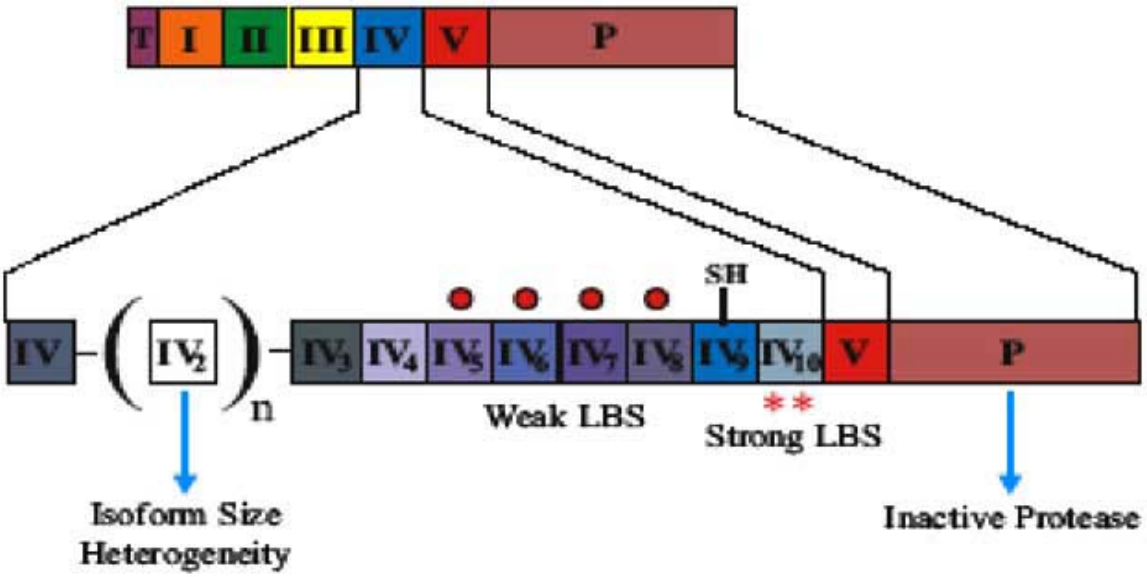

Figure 2: *Relationship between apo(a) and plasminogen:* Apo(a) lacks the N-terminal domains of plasminogen, up to and including the KIII sequence. Multiple copies of sequences similar to the KIV domain of plasminogen are seen in apo(a), and on the basis of differences in amino acid KIV sequences, can be further classified into ten types, designated $KIV_{1\text{-}10}$. All except KIV type 2 are present in single copies in the apo(a) molecule. Variability in the number of KIV_2 motifs gives rise to the Lp(a) size heterogeneity seen in the population. KIV_{10} has been shown to contain a strong lysine binding site (LBS), whereas $KIV_{5\text{-}8}$ each contains weak LBS. A single unpaired cysteine is present in KIV_9, shown by mutation studies to be the site of covalent interaction with apoB-100 in the Lp(a) particle. The protease domain of apo(a) (P) is catalytically inactive due to residue substitutions at the tissue-type plasminogen activator (tPA) cleavage site, as well as a 9-residue deletion in a conserved region near the catalytic site that potentially collapses the catalytic domain (12).

Based on their respective amino acid sequences, apo(a) kringle-IV-like domains are separated into 10 types, designated KIV_1-KIV_{10}. All except kringle IV type 2 (KIV_2) are present in single copies. Variations in the number of identically repeated KIV_2 motifs (from 3 to >30 copies) form the molecular basis of Lp(a) isoforms size heterogeneity , a hallmark of the lipoprotein (4, 5, 13-17). KIV types 5-8 each contain weak lysine binding sites (LBS); the sites in KIV types 7 and 8 have been shown to be involved in the non-covalent step of Lp(a) assembly (18). Apo(a) KIV_9 contains the sole unpaired cysteine residue in the molecule that is required for the covalent bond formation between apo(a) and apoB-100 (10, 11, 18-20)**.** The KIV_{10} domain contains a strong LBS similar to the LBS found in plasminogen KIV, and has been implicated in competitive binding to fibrin, leading to decreased plasmin activation (21-23). The protease-like domain of apo(a) is catalytically inactive due in part to a nine-residue deletion in apo(a) that falls in a region conserved between several serine proteases (12). Amino acid substitutions in the tissue-type plasminogen activator (tPA) cleavage site on apo(a) also render it unrecognizable by tPA, (21, 12). Fully mature apo(a) contains 28% carbohydrate by weight with both *O*-linked glycans as well as complex forms of *N*-linked sugars (24, 25).

Isoform size and plasma Lp(a) concentrations in individuals are inherited as an autosomal dominant trait by a major dominant gene (26, 27). The apo(a) locus comprises more than 33 alleles, encoding proteins that range from <300 kDa to >800 kDa (28). Plasma Lp(a) levels vary significantly between individuals (>1000-fold), but remain nearly constant throughout one's lifetime (29). The relative resistance of Lp(a) levels to environmental factors including diet, physical activity, and conventional lipid-lowering therapy reflects a strong genetic control of Lp(a) biosynthesis (30, 31). Factors that affects biosynthesis include, but are not limited to, apo(a) gene expression, apo(a) secretion, and Lp(a) assembly (30, 31). Approximately 90% of the variability in plasma Lp(a) concentrations is attributed to the apo(a) gene, with the isoform

size contributing approximately 60% of the variation (4) . Studies have shown that the rate of Lp(a) biosynthesis, and not Lp(a) catabolism, determines its concentration in plasma (29, 32). Plasma Lp(a) levels are generally inversely correlated with apo(a) isoform size (33, 34), although exceptions do exist (35, 36). The efficiency with which Lp(a) can be assembled extracellularly may also contribute to plasma Lp(a) levels.

1.3 Lp(a) Assembly

In the process of Lp(a) assembly, apo(a) is attached to apoB-100 via a single disulfide bond, formed between Cys^{4057} in apo(a) and Cys^{3734} in apoB-100 (11). Experiments to date have supported an extracellular Lp(a) assembly process, following the secretion of both apo(a) and apoB-100 from hepatocytes (*Figure 3*). In the two-step model of Lp(a) assembly, a high-affinity, non-covalent initial interaction occurs between the weak LBS (WLBS) in the KIV_7 and KIV_8 domains of apo(a) with the Lys^{680} and Lys^{690} residues in the amino terminus of apoB100, respectively (19, 37). This step is essential for proper Lp(a) assembly, as mutations in each or both WLBS in KIV_7 and KIV_8 reduced binding affinity between apo(a) and apoB100 (18). The addition of lysine and lysine analogues, which compete with apoB-100 for binding to the LBS in the apo(a) KIV_7 and KIV_8 domains, have also been shown to decrease Lp(a) assembly efficiency (18, 19). This non-covalent interaction coordinates both apolipoproteins into proper orientation with each other for the subsequent covalent disulfide bond formation (11).

Experiments performed by Becker and others have indicated an inverse relationship between apo(a) isoform size and Lp(a) particle formation efficiency (37). Recent studies have shown that an “open” conformation of apo(a) enhances the efficiency of covalent Lp(a) formation (38); and that smaller isoforms adopt a more “open” structure when compared to larger isoforms (37). This may be one of several factors that underlie the differences seen in plasma Lp(a) levels of differently-sized Lp(a) species.

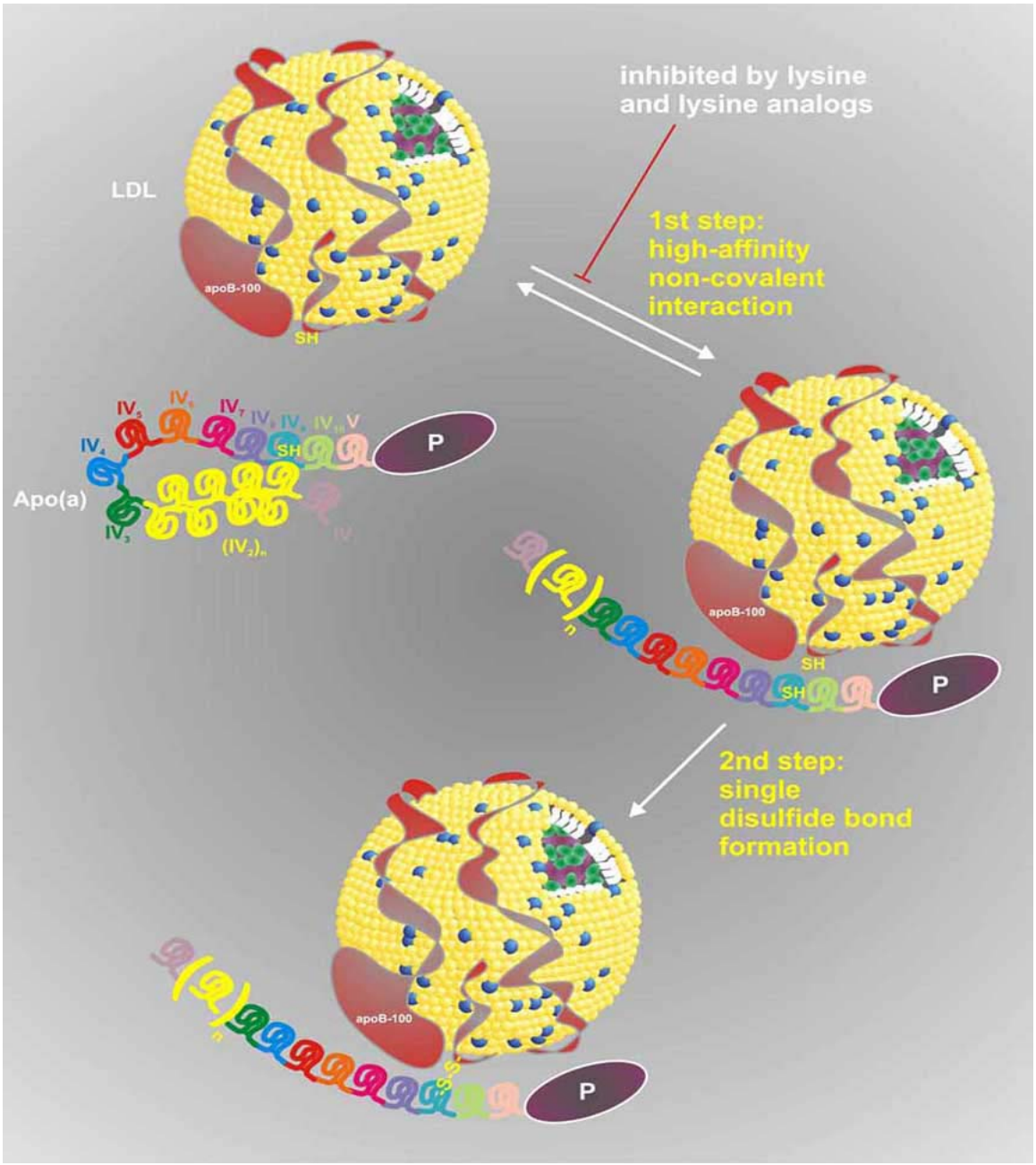

Figure 3: *Two-step model for Lp(a) assembly*. Initial high affinity, lysine-dependent interaction between KIV_{7-8} of apo(a) and the amino terminus of apoB-100 comprises the non-covalent step of assembly. Covalent disulfide bond formation then occurs between the unpaired cysteine in the apo(a) KIV_9 domain and a cysteine in the C-terminus of apoB-100. Recent results have shown that apo(a) conformation status and size may affect the covalent step of assembly (4). Modified from Koschinsky (4).

1.4 Lp(a) as a Risk Factor in Cardiovascular Diseases

Historically, clinically elevated plasma Lp(a) levels have been identified as greater than a threshold of 30mg/dL, corresponding to approximately 88nmol/L for an Lp(a) moiety containing a 17K apo(a) isoform (39). Different ethnic groups have been shown to display distinct isoform distributions and corresponding plasma Lp(a) concentrations. Overall, African Americans displayed the highest average plasma Lp(a) levels, followed by Caucasians and Hispanics in the United States (35). Another study showed that intermediate apo(a) isoform sizes (23-27K) were prominent in black Americans, whereas Caucasian Americans exhibited a more bimodal distribution in isoform size, with higher frequencies of small (<20K) and large (>30K) apo(a) isoforms (7). In addition, in individuals heterozygous for apo(a), secretion of the smaller isoforms was dependent on the size of the larger isoforms (40). Based on the presence of both an LDL as well as a plasminogen-like moiety, Lp(a) has been proposed to contribute to the process of atherothrombotic disease through both proatherogenic and prothrombotic mechanisms.

1.4.1 Proatherogenic Properties of Lp(a)

High plasma concentrations of Lp(a) have been identified as a risk factor for a variety of vascular diseases such as cerebrovascular disease and peripheral vascular disease (19, 28, 38, 8, 41-45). The majority of prospective studies performed over the past decade, however, have focused on the correlation between plasma Lp(a) levels and coronary heart disease (CHD). Lp(a) has been shown to be a powerful genetic risk factor for CHD (46), and most retrospective case-control studies have shown that patients with existing CHD have significantly higher plasma Lp(a) levels than their matched controls (4, 5, 14, 18, 19, 21, 24). A 2000 meta-analysis of 27 prospective studies, observing 5,436 CHD cases during a mean follow-up of 10 years concluded that Lp(a) is a moderate, independent risk factor for CHD (47). A more recent meta-analysis, performed using 36 long-term prospective studies published between 1970 and 2009 showed not

only a continuous correlation between Lp(a) levels an the risk of CHD, but also weak correlations between Lp(a) and several conventional vascular risk factors such as non-HDL cholesterol and apoB100 (48). Clinical studies performed by Glader and coworkers have also determined that an elevated Lp(a) levels in a cohort of northern Swedes is an independent predictor of death due to cardiovascular disease events (49).

Lp(a) has been implicated to indicate CHD risks in conjunction with other risk factors for cardiovascular diseases. A clinical study performed in Belgrade, Serbia, has indicated that patients undergoing coronary angiography, who express both low molecular weight apo(a) as well as small dense LDL, were at a significantly higher risk of developing CHD than control groups (50). This study also showed apo(a) size to be a much better indicator for CHD development than small dense LDL, although the combined effect seemed to be synergistic in nature (50). In the Quebec Cardiovascular Study, an elevated Lp(a) levels increased an individual's risk for developing ischemic heart disease in conjunction with elevated apoB and total cholesterol levels (51). The Bruneck study identified elevated plasma Lp(a) levels as a risk factor for both early (LDL-dependent) and advanced (LDL-independent) atherosclerosis, suggesting a multifaceted role for Lp(a) in different stages of atherosclerosis (52).

Elevated plasma Lp(a) concentrations have been linked with increased risks of stroke and death associated with vascular events in elderly men (53). The Prospective Study of Myocardial Infarction found that males with high LDL cholesterol were at a higher risk of myocardial infarction and angina pectoris when paired with elevated levels of Lp(a) (54). Some (55, 56) but not all (30) clinical studies in elderly women, however, have shown positive correlations between increased risks of stroke and death and elevated plasma Lp(a). Results from the Women's Heath Study indicated that extremely high plasma Lp(a) levels were an independent risk factor for future cardiovascular complications, particularly in individuals who also expressed high levels of

LDL cholesterol (55). Studies have also shown Lp(a) accumulation at the site of atherosclerotic lesions in an amount proportional to plasma concentrations (57). Apo(a) mediates Lp(a) binding to laminin, which selectively targets Lp(a) to atherosclerotic lesions, increasing the amount of LDL content in the lesions (58). The apo(a) KV region also possesses a binding site for oxidized phospholipids, targeting these atherogenic factors to lesions, and potentially increasing plaque growth (59). In this milieu, apo(a) and Lp(a) may contribute to processes that exacerbate atherosclerosis, including foam cell formation, endothelial dysfunction, inflammation, lesion calcification, and the migration and proliferation of smooth muscle cells (39, 57, 60).

1.4.2 Prothrombotic Properties of Lp(a)

Atherosclerotic plaque ruptures lead to thrombus formation, causing most CHD events associated with occlusive arterial thrombosis (61). An elevated plasma Lp(a) concentration has been implicated as a predictor for venous thromboembolism in adults, and for spontaneous and recurrent ischemic strokes in children (62-64). In the study performed by Ignatescu and colleagues, mean Lp(a) levels were significantly higher in patients with chronic thromboembolic pulmonary hypertension (65). The molecular basis of thrombotic complications due to increased Lp(a) levels stems from the striking similarity seen between apo(a) and plasminogen (12).

The active form of plasminogen, plasmin, is involved in the process of fibrin clot lysis (66). Plasminogen forms a ternary complex with tissue plasminogen activator (tPA) and fibrin, and is activated to plasmin which participates in fibrin clot lysis (66). *In vitro* and *in vivo* studies have shown anti-fibrinolytic properties of Lp(a) and apo(a), including the inhibition of both fibrin clot lysis as well as tPA-mediated plasminogen activation on fibrin surfaces (66-68). The KIV_{1-4} domains, as well as the strong LBS in the KIV_{10} motif of apo(a), have both been implicated in the inhibition of plasminogen activation (23). Previous results have suggested a simple competition between apo(a) and plasminogen for common binding sites on the fibrin or cell surface, thereby

interfering with the formation of the ternary complex (12). Recent results from our laboratory, however, support the presence of a quaternary complex in which apo(a), plasminogen, and tPA all bind to fibrin, and the efficiency of plasminogen activation is thereby decreased in the presence of apo(a) (*Figure 4*) (23, 69). A novel inhibitory role of apo(a) has also been proposed in the cleavage of fibrin-bound Glu-plasminogen to Lys-plasminogen, decreasing the zymogen's affinity to tPA (69).

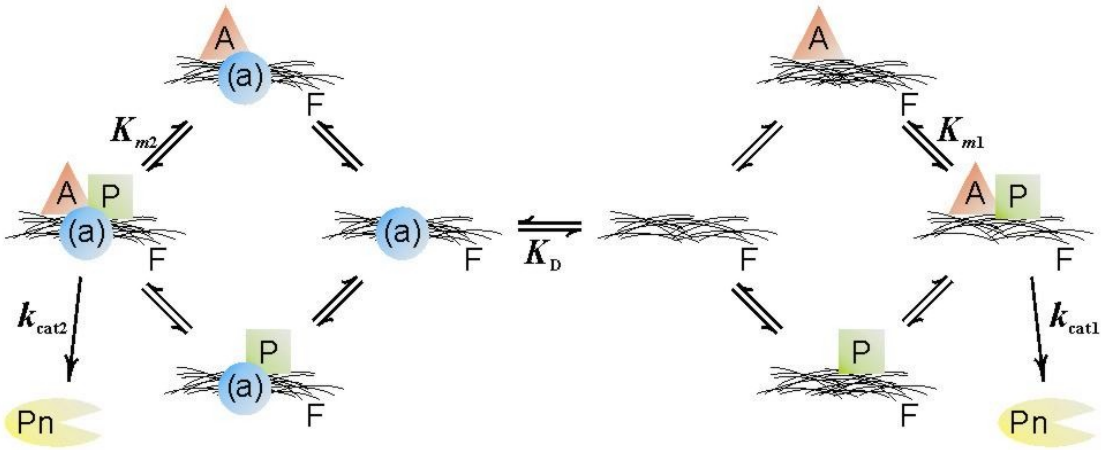

Figure 4*: Model for the inhibitory effect of apo(a) on fibrin-mediated plasminogen activation:* From right to left: The classic view of plasminogen activation includes a step-wise, separate interaction between Fibrin (F), tPA (A), and plasminogen (P), This results in a ternary complex that leads to the efficient activation of plasminogen to form plasmin (Pn) at a certain rate (k_{cat1}). Our laboratory results have shown that the inhibitory action of apo(a) ((a)) results from the formation of a quaternary complex involving fibrin, tPA, plasminogen, as well as apo(a) (see left half of figure). The efficiency of plasminogen activation is drastically decreased, in the context of the quaternary complex, leading to a reduced rate of plasmin formation (k_{cat2}) (23).

1.5 The Contribution of Apo(a) Isoform Size to CHD Risk

In vitro experiments have indicated possible apo(a) fragmentation via elastase cleavage, at a site between KIV_4 and KIV_5 (70). The amino terminal fragment has been identified in arterial lesions, while the carboxyl terminal fragment has been shown to bind to extracellular matrix components within atherosclerotic plaques (61). Overexpression of the apo(a) KIV_5-KIV_8 fragment in mice has been shown to increase overall atherosclerotic lesion area in these mice, as well as elevate plasma levels of cholesterol-rich remnant particles (70). Studies have suggested apo(a) polymorphism to be a greater indicator for CHD severity than plasma Lp(a) levels (71-73). Specifically, small apo(a) isoform sizes (<22K) have been shown to be an independent risk factor for advanced carotid atherosclerosis, acute myocardial infarction, and an increased risk for the development of angina pectoris independent of plasma Lp(a) levels (52, 74, 75). It was demonstrated that while both Lp(a) concentration and small apo(a) isoforms were predictive of angina development, only the latter remained significant in a multivariate model (76).

The Stanford 5-city prospective case-control study showed that men who have experienced myocardial infarctions or coronary deaths were more likely to express lower-molecular-weight (LMW) apo(a) (18K-20K) (77). In males expressing two different isoforms of apo(a), elevated levels of LMW apo(a) were shown to be independent predictors of coronary events and the extent of coronary lesions (78). Young Asian Indians with a positive family history of premature CHD, who were also heterozygous for the apo(a) gene, were at a significant higher risk of CHD than their homozygous counterparts (79). Elevated Lp(a) concentration, in addition to the expression of small apo(a) isoforms (<22K), has been correlated with increased risk of developing premature CHD in a young Austrian population (80). The presence of ischemic heart disease and severity of coronary lesions was also seen to correlate with elevated Lp(a) levels in children expressing small apo(a) isoforms (81).

1.6 Apo(a) Folding

The endoplasmic reticulum (ER) lumen provides an isolated environment that promotes the folding of newly synthesized transmembrane and secretory proteins. Misfolded proteins are retained in the lumen until a correct conformation is reached (82). During this time, unfolding and refolding occurs with the aid of chaperone proteins. Should a protein become irreversibly misfolded, it is targeted to the ER-associated degradation (ERAD) pathway (28). Due to its complex structure and extensive glycosylation, apo(a) requires a much longer folding period than other secretory proteins (83). Previous studies conducted to determine the influence of apo(a) isoform size on folding kinetics have yielded contradictory results (8, 41).

The peculiar species distribution of apo(a) has been a somewhat limiting factor in studying this lipoprotein both *in vitro* and *in vivo*, as standard model systems utilized in *in vivo* studies, such as the mouse and rat, do not express Lp(a) endogenously (15). Studies by White and co-workers utilized primary baboon hepatocytes expressing apo(a) species of different sizes to elucidate the influence of isoform size on the rate at which apo(a) folds (8). The smallest isoform used for these experiments displayed a molecular mass of 550 kDa, approximately the size of a 43K apo(a) isoform. Two different intracellular apo(a) moieties were identified in baboon hepatocytes for each apo(a) isoform: a lighter, precursor apo(a) (pr-apo(a)) that appears at the onset of apo(a) folding, and exhibits a mobility shift as apo(a) folds; and a mature apo(a) (m-apo(a)) form that appears later on, identical in molecular weight to the secreted apo(a) moiety. A pulse-chase experimental protocol was used to identify a specific population of intracellular apo(a) and determine their folding kinetics during the chase period, using electrophoretic mobility shifts in non-reduced apo(a) samples to display the process of folding. Experimental results showed similar folding patterns between isoforms, all taking approximately 60 minutes to reach maximum band mobility shifts. The appearance of the m-apo(a) moiety was detected at different

times for different isoforms, indicating a difference in the ER resident time of these isoforms (8). The authors suggested that all apo(a) KIV domains folded in an independent manner, and thus the number of kringles present would not influence the length of time required to fold the protein. However, since the time that the non-reduced pr-apo(a) band reached maximum mobility did not always coincide with the appearance of the m-apo(a), White and coworkers further hypothesized that not all of the KIV domains reaches a correct folding conformation during the initial process, and must undergo a cycle of folding, unfolding, and refolding in the ER (8). This second step would then be dependent on the number of KIV motifs present in the isoform, giving rise to differences in ER retention time. Inhibition of glucose trimming from *N*-linked glycans abolished the appearance of m-apo(a), but did not affect folding kinetics, indicating that apo(a) secretion is dependent on proper glucose trimming in a step downstream of apo(a) folding (84). As such, apo(a) isoforms may differ in the efficiency of processing that occurs downstream of protein folding, thus giving rise to differences in secretion efficiency (8).

In a 2003 study, Nassir and others utilized human hepatoma (HepG2) and rat hepatoma McArdle RH7777 (McA-RH7777) cell lines to determine the role of disulfide bond formation in apo(a) secretion. Their data suggested a dependence of apo(a) secretion on its isoform size, with smaller isoforms reaching a fully folded form faster than larger isoforms. This prompted the authors to suggest a sequential folding model for apo(a), where prior steps in the process are required for subsequent steps to occur (41). The range of isoforms sizes utilized in the Nassir study, however, were not representative of the observed physiological allelic distribution of apo(a) (7). Variants used in these experiments were 6K, an apo(a) variant lacking KIV_{2-4} domains; 9K, an apo(a) variant lacking the KIV_2 domain; and a 13K and a 17K isoform. The majority of comparative analyses were also performed between the 6K and 13K, only one of which is a physiologically relevant isoform. The lack of isoforms that contained different

numbers of repeats of the KIV_2 domain weakened the authors' conclusion that apo(a) folding occurred in an isoform-dependent model. With the availability of stably transformed HepG2 cell lines expressing physiologically relevant isoforms of apo(a), more experiments are required to determine a clear understanding of the influence of apo(a) isoform size on the glycopoprotein's folding kinetics.

1.7 ER-Resident Protein Interactions

Glycoproteins such as apo(a) undergo several post-translational modifications, including disulfide bond formation and glycosylation, before they can be secreted from the endoplasmic reticulum (ER). From there, these glycoproteins are further modified in the Golgi apparatus, and then transported to target areas (85). In their study on apo(a) folding, White and coworkers also determined that the appearance of the m-apo(a) isoform was size-dependent, and occurred much later than the cessation of apo(a) band mobility shift, thereby indicating processes downstream of apo(a) folding to be discriminate based on apo(a) isoform size (8). Studies have shown that apo(a) secretion efficiency is linked to its processing and exit rate from the ER (25, 84). Larger apo(a) isoforms are retained for a longer period in the ER when compared to smaller isoforms, and are proposed to undergo more complex post-translational modifications (33, 8). The specific association between apo(a) and ER-resident proteins, however, has largely not been explored with respect to isoform size. Apo(a) associates transiently with two ER chaperones, calnexin (Cnx) and glucose-related protein 78/binding protein (Grp78/BiP), via the *N*-linked glycan units in apo(a) (25). Glucose trimming of the *N*-linked glycans side chain of pr-apo(a) is essential for ER secretion, as improperly glucosylated forms of apo(a) are unable to exit the ER (84). The glucosidase inhibitor castanospermine (CST) traps premature apo(a) in a monoglucosylated form, enhancing Cnx/calreticulin(Crt)-apo(a) interactions, thereby allowing for proper folding to occur. This process, however, also sequesters apo(a) in the ER, and increases the likelihood of

cytoplasmic degradation after apo(a) dissociation from Cnx/Crt (24). To date, only a few apo(a) isoforms have been used to study protein secretion from the ER (24).

ER-resident chaperones are often categorized into several groups: Heat Shock Protein homologues and co-chaperones, lectins, and protein-specific chaperones. At least two folding catalyst groups are also present, namely the Protein Disulfide Isomerase (PDI) and Peptidyl Prolyl Isomerase (PPI) families. Apo(a) has been shown to interact with HSP homologues, lectins, as well as PDI, and the prolonged ER retention time shown previously in baboon and rat hepatocytes support interactions with these enzymes (25, 41, 85, 84). To date, however, no experiments have been performed to investigate whether different isoforms of apo(a) interact differently with these ER-resident proteins.

1.7.1 Glucose-Regulated Protein 78/Binding Protein (Grp78/BiP)

Grp78/Bip is one of the most abundant ER chaperones, and is the ER homologue of cytosolic heat shock protein HSP70 (43). Grp78 is in a large multi-protein complex that includes Grp94, PDI, and several lectin chaperones (86). Grp78 contains conserved ATPase and peptide-binding domains, as well as the highly conserved Lys-Asp-Glu-Leu (KDEL) sequence in its C-terminus, marking it as an ER-resident chaperone (87). This chaperone localizes at translocons, accessing unfolded nascent protein chains as they enter the ER (87). Grp78 recognizes and binds transiently to exposed hydrophobic residues in unfolded proteins, and catalyses the ATP-coupled folding and refolding of substrates (88). Grp78 also plays a crucial role in the unfolded protein response (UPR), binding more permanently to unglycosylated proteins when transport from the ER is blocked (89). Previous evidence have shown apo(a) to reside for a prolonged period in the ER, and evidence suggest interaction of apo(a) with Grp78 (25, 8, 41). Apo(a) interaction with Grp78 has been shown in both rat hepatoma McA-RH7777 cells expressing a 6K apo(a) variant, as well as primary baboon hepatocytes (25, 28). In both cases, the interaction was enhanced in

the presence of tunicamycin, a known *N*-linked glycosylation inhibitor (25, 28). Association between apo(a) and Grp78 was also enhanced in the presence of the reducing agent dithiothreitol (DTT), confirming the chaperone role of Grp78 on apo(a) (41).

1.7.2 Grp78 and the Unfolded Protein Response (UPR)

The UPR, as the name suggests, is a cellular self-defense mechanism activated when the ER protein functions are compromised. Under homeostatic conditions, the ER capacity is greater than, or equal to the cellular demand for ER function. In this state, Grp78 interacts and inhibits the function of three transmembrane proteins-proximal signal sensors for the three major UPR-activated pathways (43). UPR occurs when the demand for ER function overwhelms its capacity, leading to ER stress, which includes an accumulation of unfolded proteins in the lumen. The triggered release of Grp78 from the ER membrane upon UPR activation allows the chaperone to associate with unfolded proteins to aid in the folding of nascent polypeptides, as well as to prevent the formation of aggregates. The signal sensors, no longer sequestered by Grp78, activate pathways that attenuate general translation, and simultaneously induce the translation of ER-resident proteins involved in the folding process (86). Grp78 also aids in targeting irreversibly misfolded proteins to the ERAD pathway.

1.7.3 Glucose-Regulated Protein 94 (Grp94)

The ER homologue of HSP90, Grp94, is also an ER-resident chaperone that functions much like Grp78. Grp94 is proposed to bind to proteins after they have been released from Grp78 (87). In complex with Grp78 and others, Grp94 function as a dimer, providing platforms for the assembly or oligomerization of loaded protein cargo (90). No direct evidence has shown apo(a) interaction with Grp94, although as a chaperone with similar functions to Grp78, some interaction is expected between apo(a) and Grp94.

1.7.4 *N*-Linked Glycosylation and the Role of Calnexin and Calreticulin in the Process

The majority of newly-synthesized polypeptides are modified by *N*-linked glycosylation when entering the ER (*Figure 5*). The precursor $GlcNac_2Man_9Glc_3$ is added to all glycoprotein peptides, where GlcNac is N-acetylglucosamine, Man is mannose, and Glc is glucose (45). ER glucosidases I and II initially remove the two outer glucose residues, respectively (84). In this monoglucosylated form, the protein is recognized by the lectins calnexin (Cnx) or calreticulin (Crt), and is prevented from forming aggregates and degraded. Interaction with Cnx/Crt also exposes the protein moiety to the ER resident protein 57 (Erp57), an isomerase that aids in the formation of disulfide bonds. If the protein is still improperly folded, it is recognized by UDP-glucose: glycoprotein glucosyltransferase (UGGT), which uses UDP-glucose transported by a UDP-glucose/UMP exchanger from the cytosol to reglucosylate the substrate, and sequesters the substrate in the Cnx/Crt cycle (45). Once the protein is fully folded in its native conformation, glucosidase II removes the last glucose residue, releasing the moiety from the cycle. Should the protein remain in the cycle for a prolonged period due to misfolding, it is recognized by ER-α-1,2-mannosidase I, which removes a terminal mannose unit, and targets the misfolded protein to the ERAD pathway (91). *Figure 6* depicts the role of several ER-resident proteins in the Cnx/Crt cycle (91).

The lectins calnexin and calreticulin perform similar functions, modifying newly synthesized glycoproteins for transport to the Golgi apparatus (*Figure 6*) (43). Both are members of the legume lectin family, are localized in the ER, and are monomeric, calcium-binding proteins (45). Calnexin is a 90 kDa ER membrane protein, while calreticulin is a 60 kDa luminal protein. Crt is more frequently associated with soluble substrates, while Cnx associates with both

membrane-bound and soluble proteins. Substrates for Cnx and Crt mostly overlap with one another, with a few specific exceptions, however physically exchanging the location of the two lectins (converting Cnx into a luminal protein, and Crt into a membrane-bound protein) appears to swap their substrate specificities (88, 92). Structural analysis suggests that substrates bind in the space between the curved P-domain arm and the globular region in both lectins, which shields the substrate from external factors and other incompletely folded proteins (93, 94).

The precursor form of apo(a) has been shown to interact with both Cnx and Crt, as would be expected for a highly glycosylated protein such as apo(a). In mice hepatocytes stably expressing a 17K apo(a) isoform, interaction between pr-apo(a) and the two lectins was maintained for the same length of time that apo(a) required to reach a stable folding conformation, indicating a folding chaperone role of Cnx and Crt for apo(a) (84). Enhanced interactions between Cnx and apo(a) via trapping apo(a) in a monoglucosylated form in baboon hepatocytes sequestered the glycoprotein in the ER, with the abolishment of both proteolytic degradation and secretion under these conditions (28).

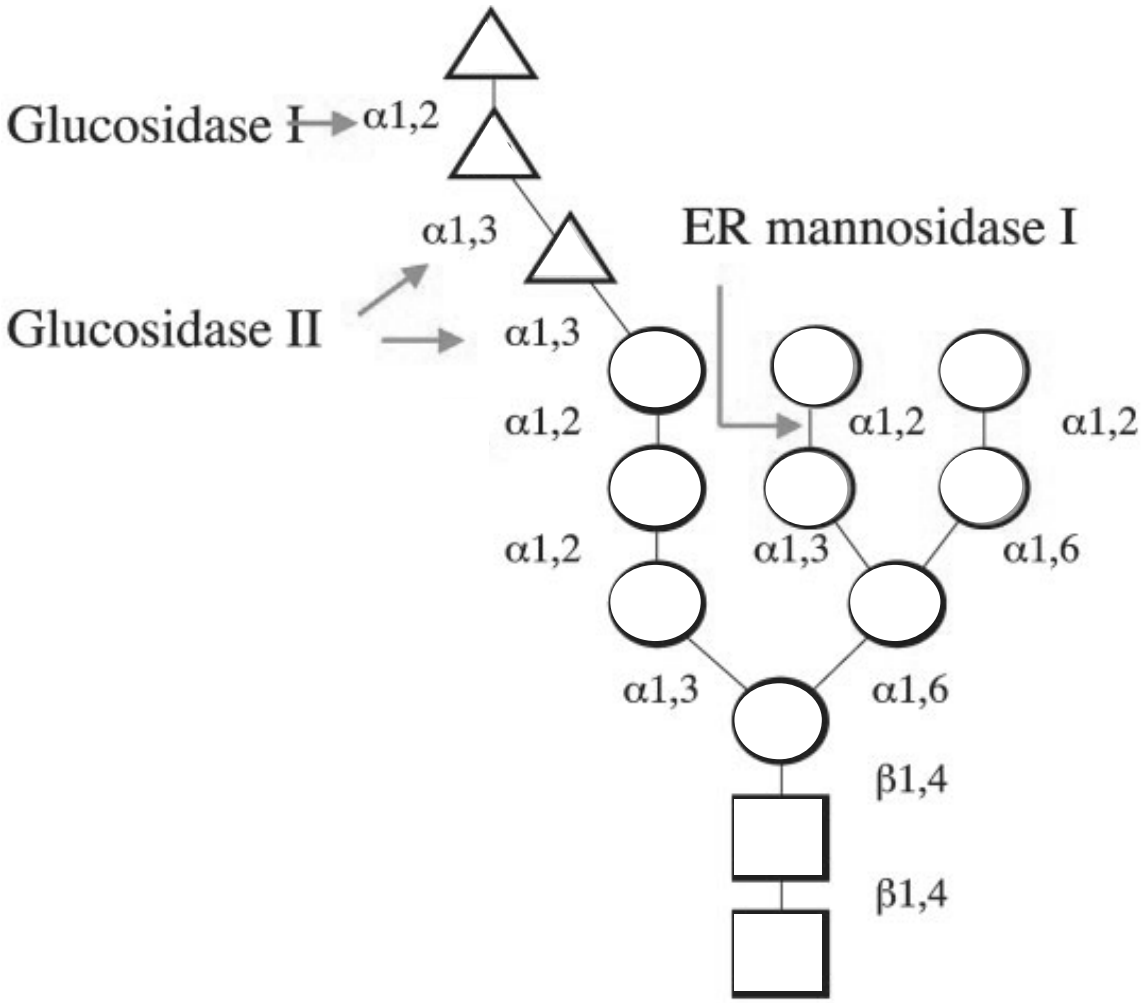

Figure 5*: The N-linked glycan core*: The core glycan contains 14 saccharides: 3 Glucose (Triangles), 9 Mannose (Circles), and 2 N-Acetylglucosamine (Squares). The trimming locations by some glycosidases are as indicated. Modified from Helenius and Aebi (45).

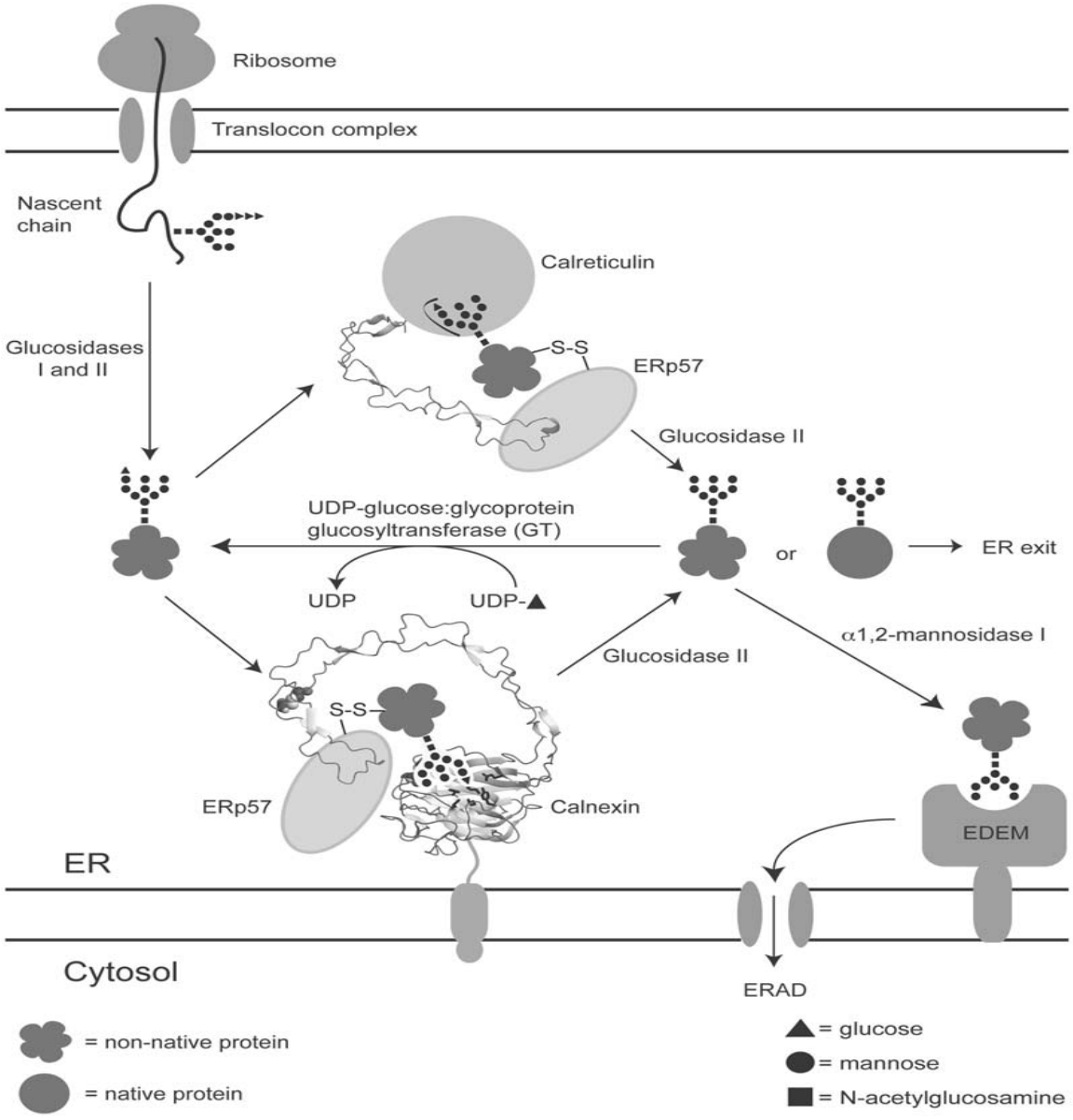

Figure 6*: The Calnexin/Calreticulin Cycle:* After the outer two glucose moieties are removed by glucosidase I and II, monoglucosylated glycoprotein is recognized by calnexin (Cnx) or calreticulin (Crt) and enters the cycle. Exposure to Erp57, a thiol-disulfide oxidoreductase, allows for disulfide bond formation and isomerization. Removal of the last glucose by Glucosidase II dissociates the glycoprotein from Cnx/Crt, shuttling the glycoproteins into one of three pathways. Properly folded proteins are transported out of the ER for further modifications. Improperly folded proteins are reglucosylated by UDP-Glc: glycoprotein glucosyltransferase (UGGT). The substrate reassociates with Cnx and Crt. Finally, ER mannosidase I removes a terminal mannose from the glycan chain of irreversibly misfolded proteins, targeting them to EDEM, and subsequent transport out of the ER for ER-associated degradation. Modified from Ellgaard and Frickel (91).

1.7.5 ER-Associated Degradation (ERAD)

The ERAD process selectively eliminates misfolded proteins or unassembled protein units through proteasomal degradation (95). Substrates are initially recognized as irreversibly misfolded proteins by several enzymes, including Grp78, EDEM, and PDI (93, 95). The translocon complex then retrotranslocates these substrates from the ER to the cytosol. Finally, substrates are conjugated with ubiquitin, and subsequently degraded via proteasomal degradation (96).

The isoform-dependent ER retention time of apo(a), coupled with low secretion levels of larger apo(a) isoforms, suggest a role of presecretory degradation in the inverse trend seen between apo(a) size and secretion efficiency. The proteasome pathway is proposed to mediate apo(a) degradation in baboon hepatocytes, and this degradation can be inhibited by Brefeldin A, which blocks ER to Golgi transport (28). Inhibitors of calpain and other cytoplasmic proteasomes have also been shown to increase both intracellular apo(a) levels, as well as apo(a) secretion efficiency in baboon hepatocytes (28).

1.7.6 ER-Associated Degradation-Enhancing α-Mannosidase-like Protein (EDEM)

Glycoproteins undergoing numerous cycles in the Cnx/Crt system without achieving complete folding are eventually subjected to terminal mannose trimming by ER α-1, 2 mannosidase, and targeted to EDEM (96). A membrane protein that is homologous to ER mannosidase I, EDEM lacks any α 1,2-mannose processing abilities, and has been shown to interact with calnexin, but not calreticulin (*Figure 6*) (43, 45, 97). EDEM interaction with proteins releases them from Cnx, removing irreversibly misfolded or unassembled polypeptides from the Cnx/Crt cycle into the ERAD pathway. EDEM is also upregulated in the event of UPR activation, aiding in the clearance of misfolded proteins in the ER (43, 96). Previous studies have

indicated that apo(a) undergoes the Cnx/Crt cycle, and is also degraded via proteasomal degradation, and thus would suggest a role for EDEM in linking the two processes (28, 84).

1.7.7 Protein Disulfide Isomerase (PDI)

PDI belongs to a family of thiol oxidoreductases of the same name (98). PDI contains four thioredoxin motifs, catalyzing the formation of disulfide bonds in nascent proteins (98). As its name suggests, PDI also isomerizes misaligned disulfide bonds to properly aligned ones (98). In addition, PDI has been shown to specifically interact with disulfide-free, misfolded secretory proteins (99). The redox activity of PDI is governed by its CXXC active site. In its oxidized state, the disulfide is transferred from PDI to the substrate, and vice versa (98). PDI has been shown to interact with apo(a) in baboon hepatocytes, and its interaction with apo(a) after apparent folding completion supports the unfolding and refolding cycle hypothesis put forth by White and colleagues for rationalizing the discrepancy seen between apo(a) folding kinetics and secretion with respect to isoform size (36).

1.7.8 ER Resident Protein 57 (Erp57/Grp58)

Erp57 is another PDI family protein that interacts specifically with newly synthesized glycoproteins, complex with Cnx/Crt in the lectin-mediated protein folding cycle, as discussed above (*Figure 6*). Erp57 also contains four thioredoxin motifs, acting as a thiol oxidoreductase to catalyze disulfide bond formation (91). Deletion mutation studies have identified Erp57 interacting with the distal region in the P-domain of Cnx and Crt (100, 101). This then further sequesters protein substrates in the P-domain curve, allowing Erp57 to catalyze disulfide bond exchanges in an attempt to aid the protein in reaching a fully folded conformation. Apo(a), as a glycoprotein, is expected to interact with Erp57 in the ER, although no studies have been performed to explore this chaperone's role in intracellular apo(a) processes.

1.8 Apo(a) Intracellular Degradation

Several intracellular degradation pathways occur in cells; the most characterized being ERAD-associated proteasomal degradation (28). This proteolytic degradation via ubiquitination occurs in two steps. The E1 enzymes activate and covalently attach an initial ubiquitin to an ε-NH_2 group of an internal lysine residue, or to a general α-NH_2 group of the substrate. Subsequent additions by the E2 and E3 enzymes bind ubiquitin moieties to an internal lysine residue in the conjugated ubiquitin. Once polyubiquitinated, the cytosolic 26S proteasome degrades the substrate, and recycles ubiquitin via ubiquitin C-terminal hydrolase (102).

While different apo(a) isoforms are translated at similar rates in baboon hepatocytes, the secretion level of larger isoforms is much lower than that of smaller isoforms (36). This is, in part, due to the level of ER-associated presecretory degradation that occurs to the maturing apo(a) protein as it travels to the cell membrane (28). Experiments published to date have supported a proteasome-mediated degradation pathway (28, 84, 103). The 26S proteasome inhibitor was shown to increase the secretion of large, low secretory level apo(a) isoforms (103). Ubiquitination was also seen on some apo(a) precursors inside the ER lumen, targeting the premature apo(a) for proteasomal degradation (28). Inhibition of the cytosolic proteasome calpain activity has been shown to increase intracellular apo(a) levels in mice hepatocytes (28). The sequestration of apo(a) in its monoglucosylated form by CST, a UGGT and glucosidase inhibitor (see *Figure 6*), traps apo(a) in the Cnx/Crt cycle, and has been shown to increase intracellular apo(a) content (84). Furthermore, studies blocking the ER-Golgi transport with Brefeldin A showed that apo(a) degradation was decreased, indicating that apo(a) must translocated out of the ER lumen for degradation (24). Apo(a) must be transported out of the ER for intracellular degradation in baboon hepatocytes (28). Therefore, intracellular apo(a) degradation may occur, in part, through the proteasomal pathway. The mechanism by which

apo(a) is degraded, and the extent to which different isoforms of apo(a) are degraded prior to secretion remains to be clarified.

1.9 Rationale and Hypothesis

Plasma Lp(a) levels have been shown to inversely correlate with apo(a) isoform size (32-34). Factors that influence this correlation include, but are not limited to, mRNA stability, translational efficiency, Lp(a) assembly efficiency, and Lp(a) catabolism (15, 32). Previous studies have shown that this inverse relationship between plasma Lp(a) levels and apo(a) isoform size is due to a role in apo(a) production and secretion, rather than the rate at which Lp(a) is catabolized (29, 32). It has also been shown *in vitro* that larger apo(a) isoforms are secreted in a relatively inefficient manner from hepatocytes (28, 33). Studies on intracellular apo(a) maturation in stably transformed HepG2 cells have found that, in cells expressing larger apo(a) isoforms, the majority of intracellular apo(a) existed in the precursor form (33). Larger isoforms of mature apo(a) required a longer period of time to appear in the Golgi apparatus than smaller isoforms, supporting the hypothesis that larger apo(a) isoforms are retained in the ER for a longer time than smaller apo(a) species (33, 104). Therefore, insight into specific differences in intracellular processing of differently-sized apo(a) isoforms may provide an explanation to the differences seen in apo(a) secretion efficiency. Studies to date have generally focused on three distinct intracellular steps with respect to apo(a) isoform size: protein folding kinetics, secretion from the ER, and presecretory protein degradation.

In order to facilitate this type of analysis, our laboratory has generated a set of apo(a) variants stably expressed in human cell lines (embryonic kidney HEK 293 and hepatoma HepG2) that span most of the physiological apo(a) allelic range (*Figure 7*), and has utilized these in an attempt to confirm and enhance present understandings of plasma Lp(a) levels with respect to apo(a) isoform size differences. HEK 293 cells are known to uptake plasmids for easy

transfection, and were demonstrated to stably express and secrete recombinant apo(a) isoforms efficiently (69). Therefore, experiments were performed in these cell lines stably expressing several different apo(a) isoforms and fragments to provide an initial understanding of the differences in intracellular processes between differently-sized apo(a) isoforms, HepG2 cells are an immortalized cell line of human hepatocytes that do not express any endogenous apo(a) (105), and therefore provide an optimal model system for studying the intracellular processes of hepatocytes. Previous experiments performed on HepG2 cells have also indicated that apo(a) size was inversely correlated with both the appearance of intracellular mature apo(a), as well as apo(a) secretion efficiency in these cells, mimicking the relationship present in human hepatocytes *in vivo* (33, 104).

This project strives to determine the differences in intracellular processes involved in the secretion of differently-sized apo(a) from human hepatocytes. Overall, we hypothesize that *plasma Lp(a) levels are dictated in part at the level of apo(a) secretion, and are attributable to isoform-dependent differences in intracellular apo(a) folding and degradation*.

1.10 Specific Aims

The present study is divided into three parts, corresponding to the major steps involved in apolipoprotein(a) secretion:

1) To identify any differences in apo(a) folding, specifically in disulfide bond formation, between apo(a) variants ranging from $KIV_{2/3}$ (containing 3 copies of the KIV_2 domain) to 30K (containing 21 KIV_2 domains) (*Figure 7*). A pulse-chase experimental protocol was utilized for these experiments, as modified from protocols developed by White et al. (8).
2) To determine differences in differently-sized apo(a) isoforms with respect to the extent of their interactions with specific ER chaperone proteins. For these studies, a pulse-chase experimental protocol, followed by co-immunoprecipitation, was performed based on the procedures of White et al. (84). Chaperone proteins included in this study were, in alphabetical order: i. Calnexin/Calreticulin (106); ii. EDEM (45); iii. Erp57 (44); iv. Grp78/BiP (41); v. Grp94 (43), and vi. PDI (98).
3) In conjunction with aim 2), to determine the role of presecretory degradation in regulating apo(a) secretion as a function of apo(a) isoform size. Initial experiments will determine the role of the proteasome pathway on secretion of differently-sized apo(a) species (28).

Chapter 2
Materials and Methods

2.1 Materials

Minimal Essential Medium (MEM) and Antibiotic-Antimycotic were from Gibco (Invitrogen Inc.; Carlsbad, CA). L-Cysteine-, L-Methionine-, and L-Glutamine-free Dulbecco's Modification of Eagle's Medium ($^{\text{L-Cys-/L-Met/L-Glut}}$DMEM) was purchased from MP Biomedicals (Solon, OH). Tissue culture dishes were from Sarstedt (Montreal, QC). Expre^{35}S^{35}S and [^{35}S]-Cysteine were purchased form PerkinElmer (Waltham, MA). *N*-ethylmalamide (NEM; Sigma-Aldrich, St. Louis, MO) was stored as a stock solution in 100% Ethanol at 300mM. Phenylmethanesulphonylfluoride (PMSF) was purchased from Sigma-Aldritch and stored as a stock solution in isopropanol at 100mM. Cycloheximide was also purchased from Sigma-Aldrich and stored at 200mM in Dimethyl Sulfoxide (DMSO). L-glutamine was also purchased from Sigma-Aldrich, and stored at 500nM in Phosphate Buffer Saline (PBS). Protein A Sepharose was purchased from GE Healthcare Lifesciences (Oakville, ON), washed and resuspended in a 1:1 ratio of beads: PBS. Amplify was also purchased from GE Healthcare. Immobilon P-Transfer membranes were purchased from Millipore (Billerica, MA). Sheep anti-human Lp(a) was purchased from Affinity Biologicals (Ancaster, ON). Rabbit anti-calnexin and anti-calreticulin were from StressGen Biotechnologies Corp. (Victoria, BC). Donkey anti-Rabbit HRP and Rabbit anti-Sheep HRP conjugates were both purchased from GE Healthcare. The calpain inhibitor ALLN was purchased from Sigma-Aldrich, and resuspended at 500µg/mL in DMSO. All other chaperone antibodies, as well as the Donkey anti-Goat HRP conjugates were purchased from Santa Cruz Biotechnology Inc. (Santa Cruz, CA). The Chemiluminescent Kit (ECL Kit)

and the Biomax High Performance Chemiluminescence Film was purchased from Amersham (GE Healthcare).

2.2 Cell Culture

Both HEK 293 and HepG2 cells were purchased from ATCC (CR-1573 and HB-8065, respectively), and cultured in 100mm dishes with MEM supplemented with 1%(v/v) antibiotic-antimycotic. HEK 293 cell culture medium was further supplemented with 5%(v/v) Fetal Bovine Serum (FBS; Hyclone, Logan, UT), while 10%(v/v) FBS (ATCC, Manassas, VA) was added to the HepG2 cell culture medium. Both cell types were split into 60mm dishes in a 1:3 ratio, and allowed to grow to confluencey before experimentation.

2.3 Recombinant Apo(a) Isoform Construction and Expression

Figure 7 depicts the set of apo(a) variants stably-expressed in HEK 293 or HepG2 cell lines utilized during our experiments. Constructs encoding different apo(a) isoform sizes (other than the 12K and 17K, the construction of which has been described elsewhere (103)), were assembled in the pRK5 expression vector as previously described (105). Briefly, a series of intermediate vectors were prepared in the pRK5 vector containing an *Eco*R1-*Xma*I fragment encoding apo(a) KIV_1-KIV_4, with a variable number of KIV_2 copy numbers. Intermediate vectors were generated by digestion of recombinant-apo(a) (r-apo(a)) expression plasmids with *Xma*I, followed by reclosure to remove all but required sequences. These vectors were partially digested with *Bam*HI to create single insertion sites within the KIV_2 vector sequence, into which KIV_2 concatomers were inserted (phage clone λa6 (5) partially digested with *Bam*HI). The complete apo(a) coding sequences were then reconstructed by sequential insertion of an *Xma*I-*Xba*I fragment from a variant of pRK5a17 (105) lacking the *Xma*I site in the multiple cloning site,

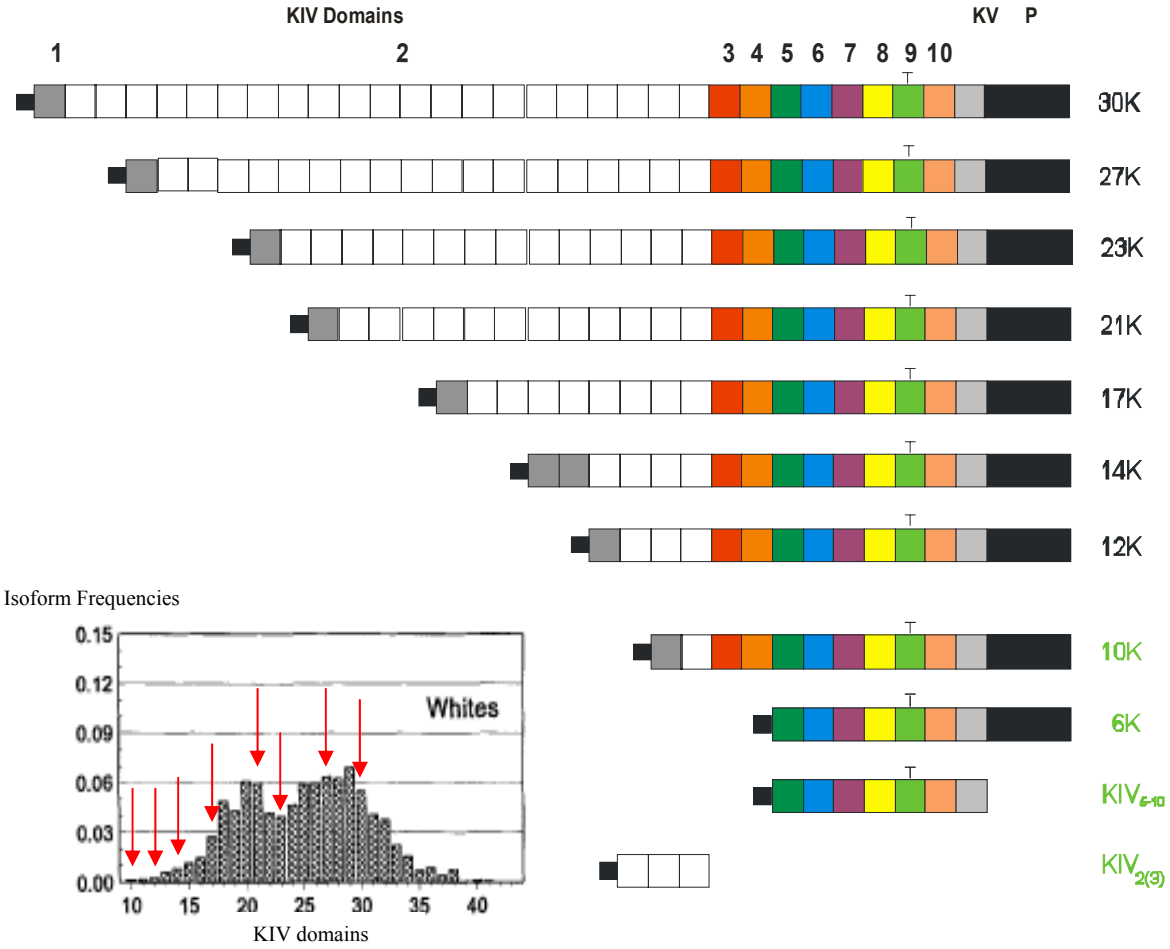

Figure 7*: Recombinant-apo(a) constructs utilized in study:* The domain structure of the full-length r-apo(a) constructs is presented at the top, where KIV and KV denote kringles related to plasminogen kringle 4 and 5 respectively, and P is the protease domain. Apo(a) contains 10 types of KIV domains (designated KIV_{1-10}), which are distinguishable from each other by small variations in amino acid sequence (107, 108). Each KIV motif is present in a single copy except for KIV_2, which is present in 3 to >30 identically repeated copies attributable to allelic variations in the number of sequences encoding KIV in the apo(a) gene (109, 110). This forms the basis of the Lp(a) size heterogeneity evident in the human population (111). Type 7 (Purple) and type 8 (Yellow) kringle domains possess weak lysine binding sites (LBS) essential in the non-covalent step of Lp(a) assembly, while KIV_9 (Green) contains an unpaired cysteine residue that is required for the covalent bond formation between apo(a) and apoB-100, depicted by the "T" above the kringle. Variants 12K to 30K represent naturally-occurring isoforms of apo(a). Modified from Feric et al. (69). *Insert*: Distribution of apo(a) alleles in a Caucasian American population. Red arrows mark the isoforms used in this study. Modified from Marcovina et al. (7).

and encompassing KIV_6 to the protease domain of apo(a), as well as an *Xma*I fragment encompassing KIV_5. All expression plasmids were used to generate corresponding stably-expressing HEK 293 cell lines as previously described (105). To distinguish the two groups, physiologically relevant apo(a) variants shall henceforth be referred to as different apo(a) isoforms, and non-physiologically relevant apo(a) variants as apo(a) fragments.

2.4 Apo(a) Folding Analysis

A pulse-chase experimental protocol was utilized to determine disulfide bond formation in differently-sized apo(a) species in HEK 293 and HepG2 cells, modified from previous protocols (*Figure 7*) (8). Duplicate experiments were performed for every variant in each cell line. Confluent cells were pre-incubated in $^{\text{L-Cys-/L-Met/L-Glut}}$DMEM supplemented with 2nM L-Glutamine for 60 minutes. Cells were subsequently pulse-labeled for one hour with Expre^{35}S^{35}S and [^{35}S]-Cysteine at a concentration of 125μCi/mL. Dithiothreitol (DTT) (5mM) was added to cell medium for the last 5 minutes of the pulse period, to reduce disulfide bonds in all newly-synthesized polypeptides. Cells were washed with Phosphate Buffer Saline (PBS), and subsequently chased in the presence of complete culture medium containing 0.5mM cycloheximide, an effective translation inhibitor. HEK 293 cells were chased for 12 minutes, during which time samples were harvested in 3-minute intervals; while HepG2 cells were chased for at least 120 minutes. 1mL each of cell medium and cell lysates were collected at each time point. To harvest lysate, cells were washed twice with ice-cold PBS containing 20mM NEM to preserve apo(a) in its various folded intermediates, and then lysed in 1mL of Extraction Buffer (50mM Tris, 150mM NaCl, 1% Nonidet P-40, 20mM NEM, pH 9.0) containing 20mM NEM and 1mM PMSF, a serine protease inhibitor. Samples were centrifuged at 8,000rpm for 5 minutes

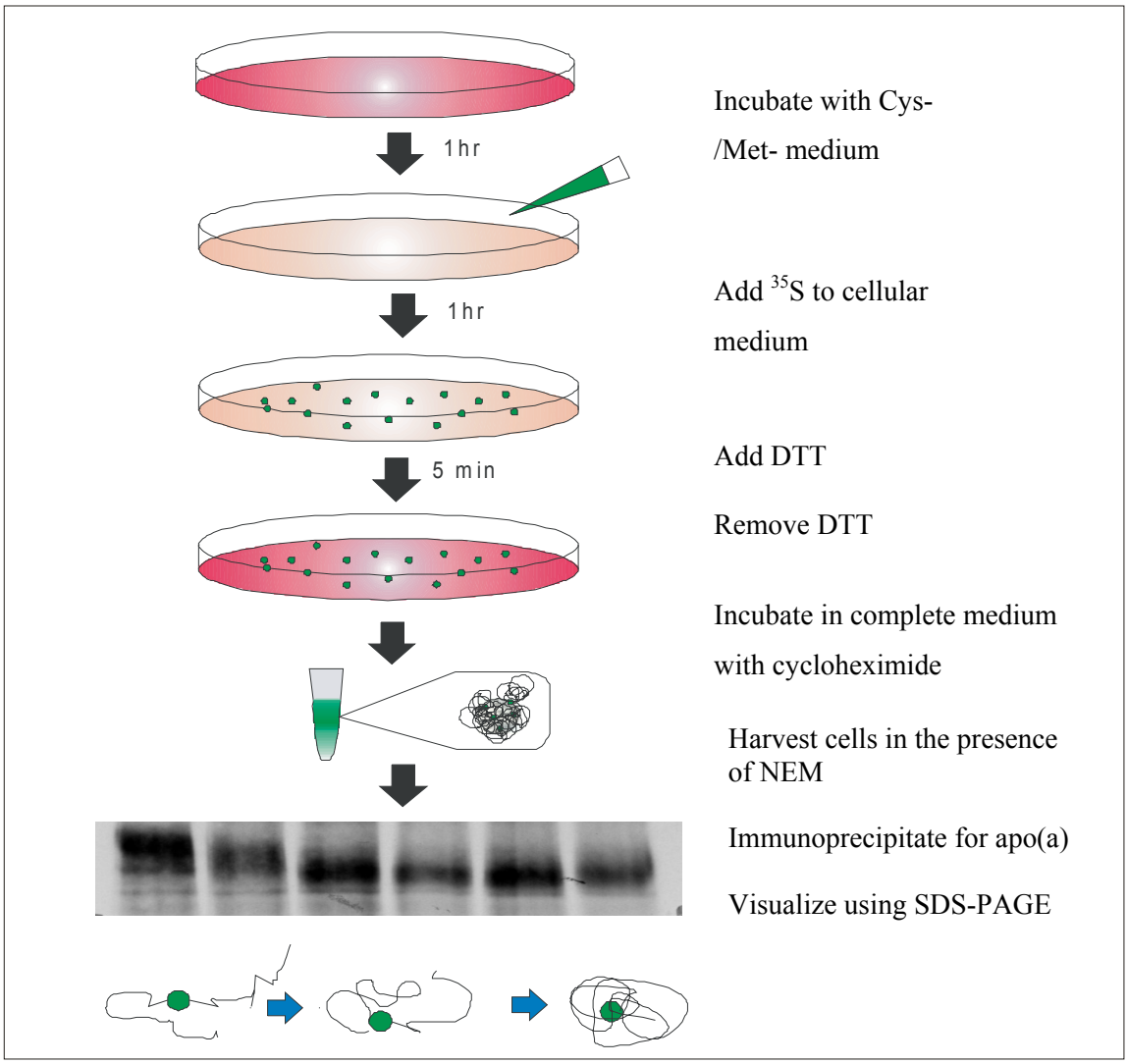

Figure 8*: Schematic overview of the apo(a) folding assay:* Disulfide bond formation were determined in HEK 293 and HepG2 cell lines using a metabolic labeling/pulse-chase procedure modified from previous protocols (8). Cells were incubated in complete medium lacking methionine and cysteine for one hour, and then labeled for another hour with 125µCi/mL each of [^{35}S]-cysteine and Expre^{35}S^{35}S label. DTT was added to reduce newly-synthesized proteins, and subsequently removed at the onset of the chase period. Cells were chased in the presence of 0.5mM cycloheximide, and harvested at time points in the presence of 20mM NEM. Apo(a) was immunoprecipitated using an anti-Lp(a) polyclonal antibody and Protein A Sepharose beads. Immunoprecipitates were then analysed using SDS-PAGE gels containing 5% to 8% polyacrylamide, in the presence (reduced) or absence (non-reduced) of DTT. Non-reduced samples depict the progression of protein folding, indicated by increased mobility of the apo(a) band.

using an Eppendorf centrifuge and the pellet discarded.

2.5 Apo(a) Immunoprecipitation

All samples were pre-cleared at room temperature using 75µL of a 50% Protein A Sepharose suspension in PBS for one hour, and spun in an Eppendorf centrifuge at 10,000rpm for 5 minutes. Supernatants from each sample were subsequently incubated overnight on a rotating shaker at 4^0C with mouse anti-Lp(a) antibody at 1µg/mL. 100µL of Protein-A Sepharose was added to each sample, and samples were then incubated for at least 1 hour at room temperature. Pellets were washed twice with RIPA Buffer (50mM Tris, pH 7.4, 0.15M NaCl, 1% Nonidet P-40, 1% Sodium Deoxycholate, 0.1% SDS, pH 7.5) containing 0.5M NaCl, once with TE Buffer (10mM Tris-HCl, pH 7.5 containing 10mM EDTA), and finally resuspended in 100µL of Laemmli Sample Buffer (112) with (reduced samples) or without (non-reduced samples) 10mM DTT, and stored at -20^0C.

2.6 Apo(a) Secretion Kinetics in HepG2 cells

To determine the appearance of apo(a) in the conditioned medium of HepG2 cells, a modified experimental design was utilized. Cells were pulse-labelled as previously described, with no DTT addition at the end of the pulse period, and then chased for 5 hours; samples were taken at various time points. Cell medium and lysates (1mL of each) were harvested, immunoprecipitated using an apo(a) antibody, and stored as described above prior to SDS-PAGE analysis. Duplicate experiments were performed for each isoform in both cell lines.

2.7 Apo(a)-ER Resident Protein Association Assay

A modified pulse-chase experimental protocol was utilized to determine apo(a) association with various chaperones and other ER-resident proteins in HepG2 cells (84). Cells

were pulse-labelled as described above, and chased for 60-120 minutes in serum-free medium. No DTT was added at the onset of the chase period. Pre-cleared samples were incubated for 3 hours at 4^0C with an antibody specific to the chaperone of interest, and subsequently immunoprecipitated for 2 hours with 100µL of Protein-A Sepharose suspension at room temperature. Pellets were washed 3 times for 5 minutes at 4^0C with association buffer (AS) (50mM HEPES, pH 7.4 containing 0.3% CHAPS and 200nM NaCl), and then eluted by boiling for 10 minutes at 100^0C in the presence of 100µL Elution Buffer (AS containing 10mM EDTA and 1% Triton X-100). Supernatants were subsequently diluted 10-fold in dilution buffer (50mM Tris, pH 9.0 containing 0.3% CHAPS, 100mM NaCl and 1% Triton X-100), and incubated overnight at 4^0C on a rotating shaker with anti-Lp(a) antibody. Following immunoprecipitation, samples were resuspended in Laemmli sample buffer containing 10mM DTT. Experiments were performed in duplicates.

2.8 Apo(a) Intracellular Degradation Inhibition Assay

Apo(a) degradation was studied using a modified protocol previously described by White and colleagues (28). Cells were pulsed and chased as described for the apo(a) folding assay (see section 2.4 above) with the addition of 5ug/mL ALLN to experimental plates (Treated) at the onset of the chase period. No DTT was added at the end of the pulse period. Samples were immunoprecipitated as described above, and resuspended in Laemmli Sample Buffer containing 10mM DTT. Experiments were performed in duplicates for all isoforms.

2.9 SDS-Polyacrylamide Gel Electrophoresis (PAGE) and Immunoblotting

Apo(a) visualization was performed as previously described (10, 113). Samples were denatured at 100^0C for 10 minutes prior to gel electrophoresis, and 7-10µL of samples was loaded into each well. Purified recombinant apo(a) proteins were run alongside samples to identify

apo(a) bands in the gels. The percentage of acrylamide in the gels was adjusted according to the apo(a) variant size: 8% polyacrylamide was used for the $K(IV_2)_3$ concatomer, KIV_{5-10}, and 6K fragments; 7% for 10K and 12K apo(a), 6% for 14K to 21K isoforms, and 5% for >21K isoforms. In all cases, gels were run at 150 volts, fixed for 15 minutes with fixing solution (25% isopropanol, 10% glacial acetic acid), amplified for 30 minutes using Amplify Fluorographic Reagent, dried for 30 minutes at 75^0C under vacuum on chromatography paper, and then exposed to film for various periods at -70^0C with intensifying screens using High Performance Chemiluminescence Film.

To immunoblot for chaperones and apo(a) marker proteins, gels were run as previously described, and transferred electrophoretically to Immobilon P-Transfer Membrane at 100mA for 1 hour, then blocked overnight at 4^0C in NET (50mM Tris, , pH to 7.4 containing 0.15M NaCl, 6.4mM EDTA, and 0.05% Triton X-100) containing 8% (w/v) milk powder. Membranes were probed with the appropriate primary antibodies each at a dilution of 1:3000 in NET for one hour, followed by four 15 minute washes with NET. Secondary antibodies with HRP Conjugates were added at a dilution of 1:3000 in NET for one hour, also followed by four washes. Bands were visualized using an ECL kit and exposed to film for a period of 15 seconds to 2 minutes.

2.10 Apo(a) Folding Assay: Band Shift Distance Quantification

The distances migrated by the apo(a) bands at various time points during the chase period were analysed using autoradiograms of non-reduced apo(a) folding gels with ImageJ software. A reference band was chosen, using either the two sets of protein markers available on the gel, or a non-specific band that appeared in all lanes. The optical density of each lane was plotted, and distance was measured between the apo(a) band and the reference band. The absolute distance migrated was defined as the difference between the distance traveled by the apo(a) band at a

given time point compared to the position of the apo(a) band at time 0. The percentage shift in band mobility was then determined by dividing the absolute distance migrated by the apo(a) band by the total distance migrated by the band.

Chapter 3
Results

3.1 Analysis of Apolipoprotein(a) Folding

Previous attempts at elucidating apo(a) folding kinetics have yielded contradictory results, showing that the kringle domains fold either in a simultaneous (8) or a sequential process (41, 8). Our laboratory has since generated a set of stably-transformed human cell lines in HEK 293 cells and HepG2 cells expressing variants of apo(a) that span most of the naturally-occurring apo(a) isoform range *(Figure 7*). We performed experiments to determine the extent of apo(a) disulfide bond formation as a function of time using the mobility of the protein in non-reducing SDS-PAGE gels as an indicator (8). Apo(a) species that have formed more disulfide bonds is theoretically more compact in size, and therefore would migrate with a greater mobility on SDS-PAGE when compared to less folded apo(a) species. Three sets of samples were prepared for each experiment: 'Lysate Non-Reduced', to visualize the formation of disulfide bonds in apo(a) species; 'Lysate Reduced', produced by the addition of 10mM DTT to the samples, and used to ensure that all lanes contain the same apo(a) isoform; and 'Cell Medium', also with 10mM DTT in the sample, to approximate the length of time required for apo(a) to exit the cell.

3.1.1 Apo(a) Folding in HEK 293 Cells

Initial experimentation indicated rapid disulfide bond formation of apo(a) in HEK 293 cells, and so a 12-minute time course was adopted, with sample collection performed in three-minute intervals. Samples were precleared, immunoprecipitated, and apo(a) bands identified via SDS-PAGE as outlined in the Materials and Methods section. *Figure 9a* shows autoradiograms of non-reduced and reduced samples of seven radiolabelled apo(a) variants analyzed for protein folding. Non-reduced samples are seen on the left, and show the progression of disulfide bond

formation through changes in band mobility. Reduced samples are seen on the right, confirming the presence of the same-sized apo(a) variants in all lanes of the same gel, The reduced samples also show changes in band mobility that are not attributed to folding. Physiologically relevant isoforms are labeled in black, the smallest one being 12K apo(a). Non-physiologically relevant fragments are labeled in green. *Figure 9b* shows the quantified distance each apo(a) band has migrated at a given time point compared to the total distance that apo(a) isoform has migrated over the 12-minute period. An overall isoform-dependent folding pattern was seen, with larger isoforms exhibiting band mobility changes at later time points than smaller isoforms. Smaller apo(a) fragments (KIV_{5-10} and 6K) and the 12K and 14K isoforms displayed large, distinct increases in protein mobility between 0 and 3 minutes, with little further changes in mobility at later time points, suggesting that these isoforms folded completely within the first 3 minutes of the chase period. On the other hand, the large, 30K isoform exhibited a much slower mobility pattern, with a change in band mobility at a point later than 6 minutes into the chase period. Interestingly, the 17K isoform appeared to fold at a continuous rate during the 12 minute sample collection time frame. Graphical analysis of band mobility change data shows a steady decrease in slope (and therefore percentage change in band mobility), with increasing apo(a) isoform size. This supports slower folding with larger apo(a) isoforms.

3.1.2 Apo(a) Folding in HepG2 Cells

In studies by other investigators, apo(a) folding in baboon and rat hepatocytes were observed over a 1-2 hour chase time (8, 41), and so a 60-minute chase time was adopted for investigating disulfide bond formation in apo(a) in HepG2 cells. An endpoint of 120 minutes was also adopted later on during the experimentation process. *Figure 10a* shows autoradiograms of non-reduced samples (left) and reduced samples (right) corresponding to seven apo(a) variants and isoforms. *Figure 10b* shows the quantified band migration distances at each time point for

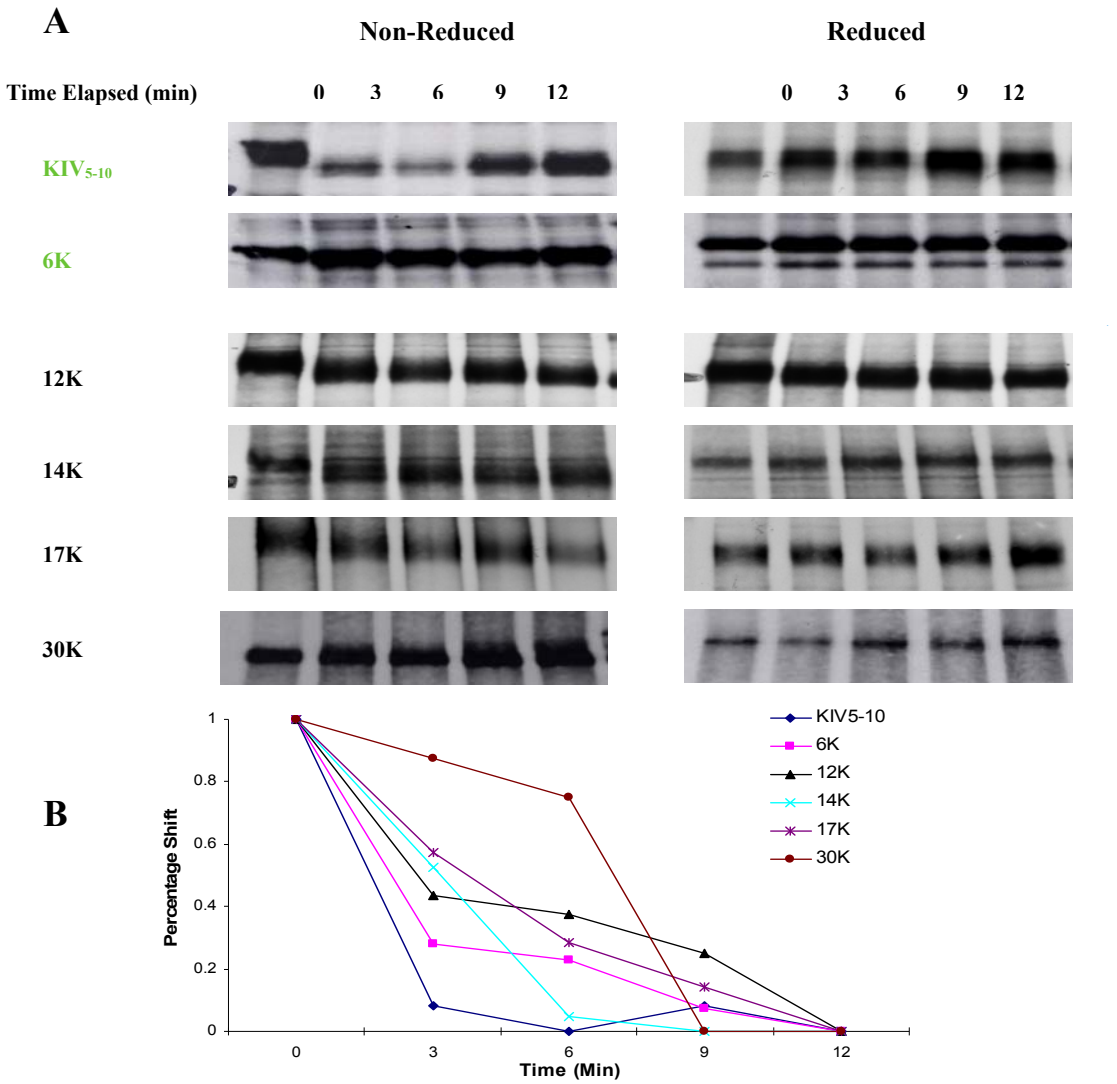

Figure 9*: Apo(a) folding patterns in HEK 293 Cells:* Cells were exposed to 0.5mM cycloheximide in serum-free medium at the start of the chase period (0 min), and subsequently collected in three-minute intervals. *A) Qualitative analysis of apo(a) band mobility changes:* Samples were analyzed by SDS-PAGE using polyacrylamide gels ranging between 5% to 7% polyacrylamide, fixed, amplified, dried, and subsequently exposed to film for a variable amount of time. Non-physiologically relevant apo(a) fragments are labeled in green, and physiologically-relevant apo(a) isoforms are labeled in black. Non-reduced gels (left) indicate that larger isoforms display downward shifts in apo(a) bands at a later time than smaller isoforms (compare 12K and 30K). Reduced gels (right) ensure that lanes being compared contain the same apo(a) isoform. *B) Quantitative analysis of apo(a) band mobility changes:* percentage shift was determined by comparing the distance traveled by the apo(a) band at each time point compared to the overall distance traveled by the apo(a) isoform over the 12-minute period using the ImageJ software. Taken together, the data suggests that apo(a) folds in an isoform-dependent manner in HEK 293 cells. Data are representative of duplicate experiments.

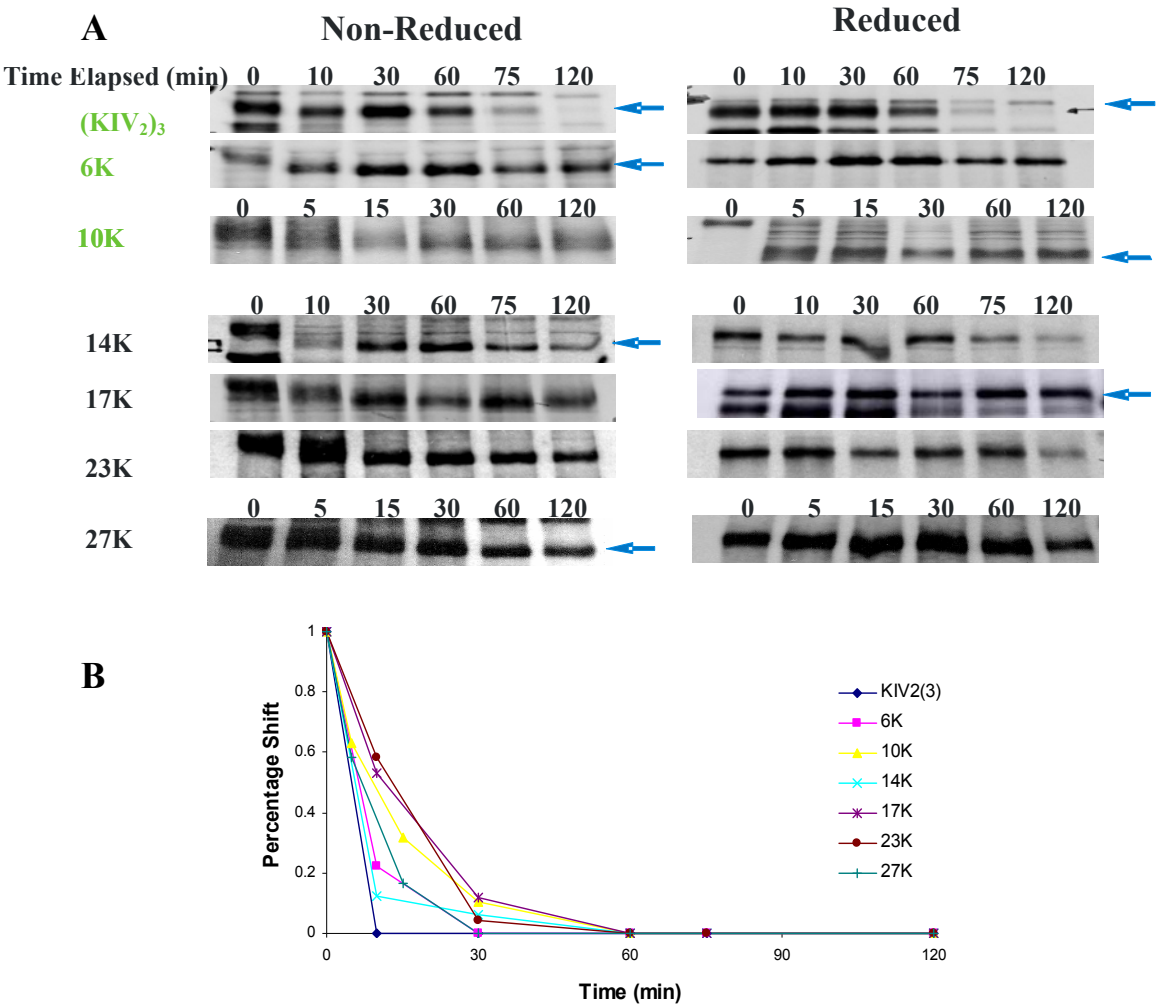

Figure 10: *Apo(a) folding patterns in HepG2 Cells:* Cells were exposed to 0.5mM cycloheximide in serum-free medium at the start of the chase period (0 min) and subsequently collected. Two different time point intervals were utilized: cells expressing 10K and 27K apo(a) were harvested at 0, 5, 15, 30, 60, and 120 minutes into the chase period, while other variants were collected at 0, 10, 30, 60, 75, and 120 minutes after the commencement of the chase period. *A) Qualitative analysis of apo(a) band mobility changes:* Samples were analyzed by SDS-PAGE using polyacrylamide gels ranging between 5% to 8% polyacrylamide, fixed, amplified, dried, and subsequently exposed to film for a variable amount of time. Apo(a) fragments tested appeared to fold in a size-dependent manner. All physiologically relevant apo(a) isoforms tested (>14K) appeared to achieve a fully folded conformation after 60 minutes. Arrows indicate the apo(a) species when multiple bands are visible. *B) Quantitative analysis of apo(a) band mobility changes:* percentage shift was determined by comparing the distance traveled by the apo(a) band at each time point compared to the overall distance traveled by the apo(a) isoform over the 120-minute period using the ImageJ software. Taken together, our data suggests that apo(a) folds in an isoform-independent manner in HepG2 cells, with different isoforms sizes achieving a fully folded conformations in approximately the same amount of time.

each apo(a) isoform as a percent of the total change in band mobility exhibited by apo(a) over the 120 minute chase period. Two different time courses were performed, one with 3 time points in the first 60 minutes of the chase period, and a modified time course with 4 time points in later experiments to gain a clearer disulfide bond formation profile during the first 60-minute period. Smaller apo(a) fragments showed isoform size-dependency in the time required for reaching maximum band shift. The smallest fragment, a concatomer of three apo(a) KIV_2 domains, only showed band shift in the first 10 minutes of the chase period. The 6K isoform, containing a chimera of KIV types 1 and 5 of apo(a), followed by the $KIV_{6\text{-}10}$, KV, and P domains, showed increases in band mobility until the 30 minute time point. The 10K isoform showed a large band mobility shift in apo(a) bands within the first 5 minutes of the chase period, followed by a steady shift until the 60 minute time point. For physiologically-relevant apo(a) isoforms (>14K), our results showed similar band shift patterns to what has been reported using primary baboon hepatocytes (8). Our data suggests that folding commences immediately after the pulse period, and increases in the mobility of bands are seen up to 60 minutes into the chase period. All isoforms, remarkably, appeared to reach a stable conformation within 60 minutes. In summary, all physiologically-relevant isoforms displayed an isoform size-independent folding pattern, with prominent band shifts occurring in the first 30 minutes of protein folding, followed by a small shift between the 30 and 60 minute time points.

3.2 Apolipoprotein(a) Secretion in HEK 293 Cells

Conditioned medium was collected from cells stably expressing apo(a) variants during folding analysis experiments (described in section 3.1.1 above) to determine whether apo(a) secretion kinetics also differed between the two cell lines. *Figure 11* shows the appearance of mature apo(a) in the HEK 293 cell medium, labeled as in *Figure 9* (refer to *Figure 9* for corresponding intracellular apo(a) folding patterns). Similar to what was previously observed for

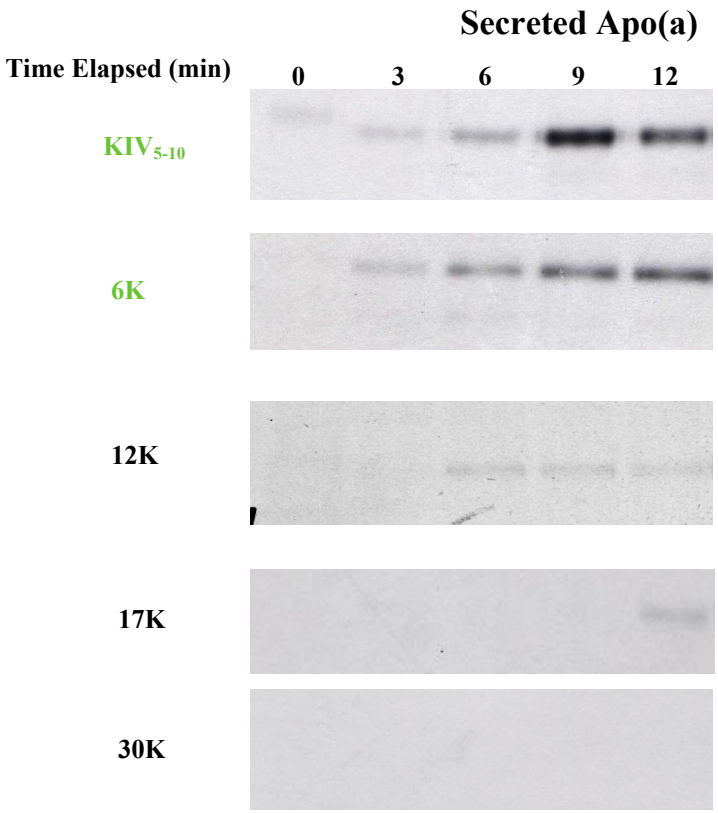

Figure 11*: Apo(a) secretion kinetics in HEK 293 cells:* Cells were metabolically labeled as previously described for the folding experiments. Samples were analyzed by SDS-PAGE using polyacrylamide gels ranging between 5% to 7% polyacrylamide, fixed, amplified, dried, and subsequently exposed to film for 72 hours. Appearance of mature apo(a) in the medium was generally correlated with a decrease in the corresponding intracellular apo(a) signals. The data collectively suggest that the rate of apo(a) secretion from HEK 293 cells appeared to be dependent on apo(a) isoform size.

apo(a) folding, larger apo(a) isoforms appeared in the medium at much later times than smaller apo(a) isoforms and fragments, with little detection of the 30K apo(a) species in the medium throughout the chase period. In most cases, the appearance of apo(a) in the conditioned medium appeared to coincide with the time at which folding was completed on the basis of the folding experiments (see *Figure* 9).

3.3 Apolipoprotein(a) Secretion in HepG2 Cells

Conditioned medium was collected from HepG2 cells stably expressing apo(a) variants during folding analysis experiments (described in section 3.1.2 above). Initial observations indicated that very little apo(a) could be detected in the conditioned medium during first 2 hours of the chase period. As such, a 5 hour time course was adopted to determine apo(a) secretion kinetics in the HepG2 cells. *Figure 12* shows the appearance of mature apo(a) in the HepG2 cell medium, labeled as in *Figure 10*. Reduced lysate samples were also collected, to confirm apo(a) production in all cell lines. In contrast to intracellular folding patterns, apo(a) secretion in HepG2 cells occurred in an isoform-dependent manner. Since no DTT was added to reduce newly synthesized apo(a) at the beginning of the chase period, the start of the chase period corresponded to the 60 minute time point of the folding kinetics time course. 10K and 14K apo(a) variants appeared in the medium approximately 30 minutes after the beginning of the chase period. The 17K isoform appeared in the medium at the 60 minute time point, while the 23K isoform could not be detected in the medium until the 120 minute time point.

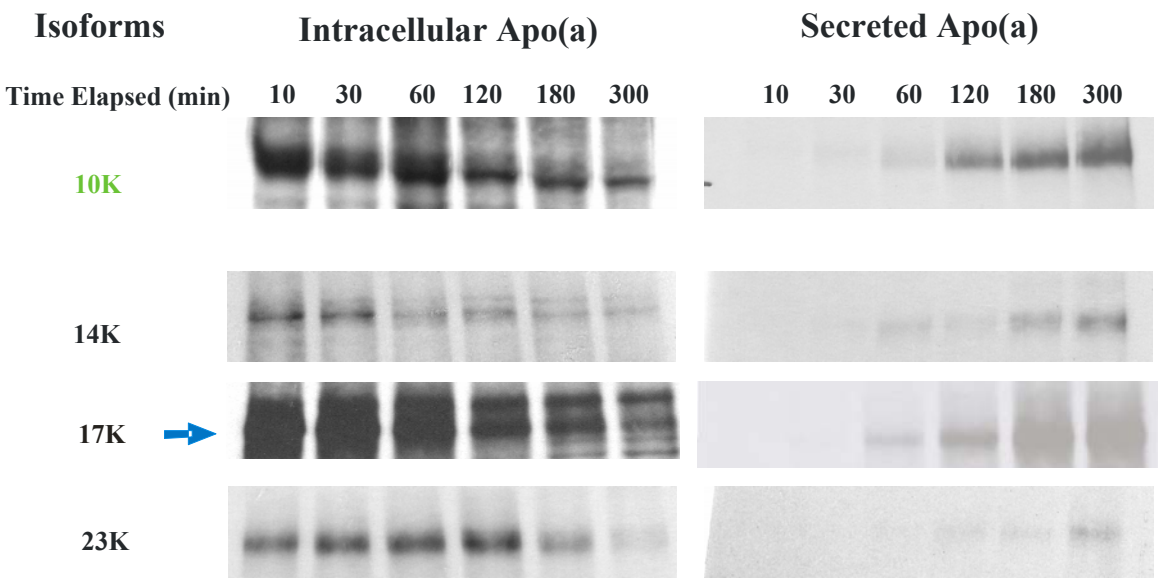

Figure 12: *Apo(a) secretion kinetics in HepG2 cells:* Cells were metabolically labeled as previously described for the folding experiments, with no addition of DTT prior to the chase period, and harvested in the presence of 20mM NEM. Samples were analyzed by SDS-PAGE using polyacrylamide gels ranging between 5% to 7% polyacrylamide, fixed, amplified, dried, and subsequently exposed to film for 72 hours. Mature apo(a) appeared earlier in the conditioned medium in the case of smaller isoforms (compare 10K with 23K). Appearance of mature apo(a) in the medium also generally corresponds with a decrease in intracellular apo(a) signals. Secretion of apo(a) from HepG2 cells appears to be dependent on isoform size.

3.4 Apolipoprotein(a) Intracellular Modifications

Eight ER-resident enzymes were studied for their interaction with intracellular apo(a), and, in this context, experiments were performed to determine the nature of these interactions as a function of apo(a) isoform size. HepG2 cells were used for these studies since they represent the most physiologically-relevant cell line for apo(a) production (33). To elucidate the nature of association between apo(a) and several ER-resident modification enzymes, a double immunoprecipitation method was used to separate enzyme-associated apo(a) from total intracellular apo(a), as described in section 2.7. Gels present in all figures are representative of duplicate experiments.

3.4.1 Apo(a) interaction with PDI

PDI is an ER-associated thiol bond exchange enzyme that associates with both newly synthesized proteins, as well as misfolded proteins, to aid in their reaching a correct final conformation. Representative gels of duplicate experiments showing the interaction between varying apo(a) isoforms and intracellular PDI are shown in *Figure 13*. The amount of total PDI present in each sample was also determined by immunoblotting as a normalization tool to ensure all samples in a set were exposed to the same amount of isomerase. Interestingly, the 10K and 14K apo(a) variants appeared to associate with PDI much longer than the larger isoforms, which all seem to dissociate between 15 and 30 minutes into the chase period. An extended chase period showed that the 14K apo(a) isoform disassociated from PDI shortly after the 60 minute chase time point, indicating that the interaction was indeed transient (data not shown).

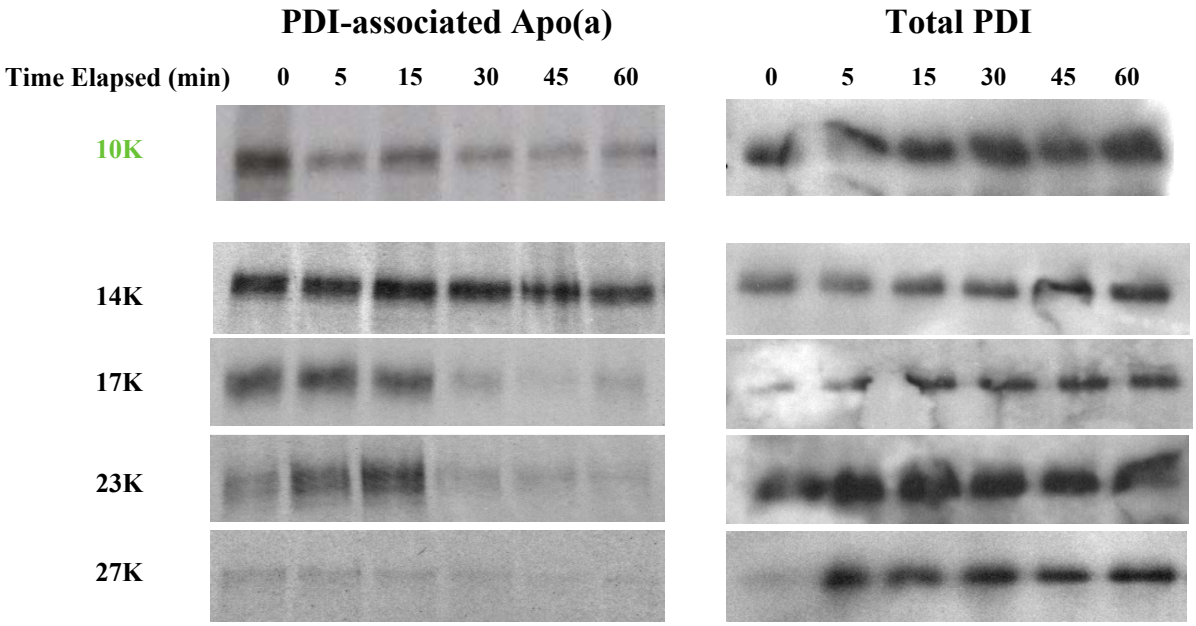

Figure 13: *Intracellular association of apo(a) with Protein Disulfide Isomerase (PDI):* Cells were metabolically labeled as previously described for determining apo(a) secretion from HepG2 cells (see section 3.1.2), with no addition of DTT prior to the chase period. The chase was performed in serum-free medium, and cells were harvested in the presence of 20mM NEM, as modified from a previous protocol (84). An initial IP was performed using an anti-PDI antibody, followed by a second IP using an antibody specific for apo(a). Samples containing PDI-associated apo(a) were analyzed by SDS-PAGE using polyacrylamide gels ranging between 5% to 7% polyacrylamide, fixed, amplified, dried, and subsequently exposed for 14 days. Total lysate PDI content was also determined via western blotting, as a normalization tool. Lysate samples were analyzed by SDS-PAGE as before, followed by immunoblotting using an anti-PDI antibody, as described in section 2.9. Gels are representative of duplicate experiments. The data suggest transient interaction of apo(a) with PDI for all variants except 10K and 14K.

3.4.2 Apo(a) interaction with Erp57

Erp57, also known as Grp58, is an ER-resident enzyme of the PDI family that interacts primarily with newly-synthesized glycoproteins (91). *Figure 14* shows representative gels of preliminary experimental results on the interaction between apo(a) and this enzyme. Association between apo(a) and Erp57 appeared to be transient, although this interaction seemed to occur at a much earlier time than PDI (compare 17K-Erp57 with the 17K-PDI association shown in *Figure 13*). The larger, 23K apo(a) isoform was seen to rapidly dissociate from Erp57 shortly after the 5 minute time point, although a basal level of association was maintained throughout the chase period. The 17K isoform of apo(a) dissociated from Erp57 at a slower rate, although complete dissociation from the enzyme was seen for this isoform at the 120 minute time point.

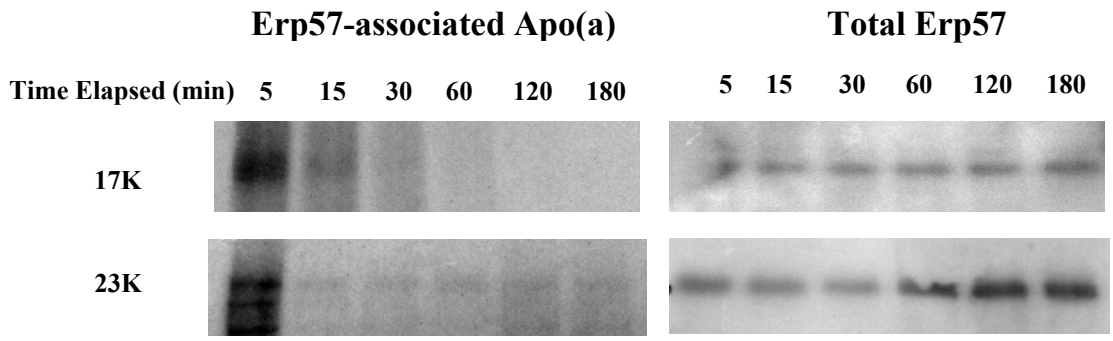

Figure 14: *Intracellular association of apo(a) with ER Resident Protein 57 (Erp57):* Cells were metabolically labeled as previously described for determining apo(a) secretion from HepG2 cells (see section 3.1.2), with no addition of DTT prior to the chase period. The chase was performed in serum-free medium, and cells were harvested in the presence of 20mM NEM, as modified from a previous protocol (84). An initial IP was performed using an anti-Erp57 antibody, followed by a second IP using an antibody specific for apo(a). Samples containing Erp57-associated apo(a) were analyzed by SDS-PAGE using polyacrylamide gels ranging between 5% to 7% polyacrylamide, fixed, amplified, dried, and subsequently exposed to film for 32 days. Total lysate Erp57 content was also determined, as a normalization tool. Lysate samples were analyzed by SDS-PAGE as before, followed by immunoblotting using an anti-Erp57 antibody, as described in section 2.9. Gels are representative of duplicate experiments. Current experimental data suggest interaction of apo(a) with Erp57 occurs in a transient manner.

3.4.3 Apo(a) interaction with Calnexin

Calnexin, along with calreticulin, are ER-resident lectins that mediate proper glycosylation of proteins before exit from the ER. Calnexin is localized on the cytosolic surface of the ER, whereas calreticulin is strictly a luminal enzyme. Both form a complex that includes Erp57 as well as the catalyst UGGT, and ensure that newly synthesized glycoproteins are properly folded and glycosylated before their exit from the ER. Apo(a) interaction with calnexin can be clearly seen in *Figure 15*. Interaction appeared to be transient between calnexin and the 17K and 23K apo(a) isoforms. 17K apo(a) appeared to associate with calnexin within the first 5 minutes of the chase period, and dissociated between the 60 and 120 minute time points. The 23K apo(a) isoform also appeared to associate with calnexin at the onset of the chase period, and dissociated from the lectin sometime after the 120 minute time point. The interaction between calnexin and the 14K apo(a) isoform appeared to be continuous. No persistent trend in calnexin association with differently-sized apo(a) isoforms is currently present in our data.

3.4.4 Apo(a) interaction with Grp78

The ER resident protein Grp78 recognizes and binds to exposed hydrophobic residues in the unfolded regions of proteins. The interaction between the 17K apo(a) isoform and Grp78 is shown in *Figure 16*. Significant association appeared to occur early in the chase period, although a continuous basal association persisted throughout the 120 minute chase period between apo(a) and Grp78. Grp78 association with other isoforms must be performed before any other conclusions can be drawn.

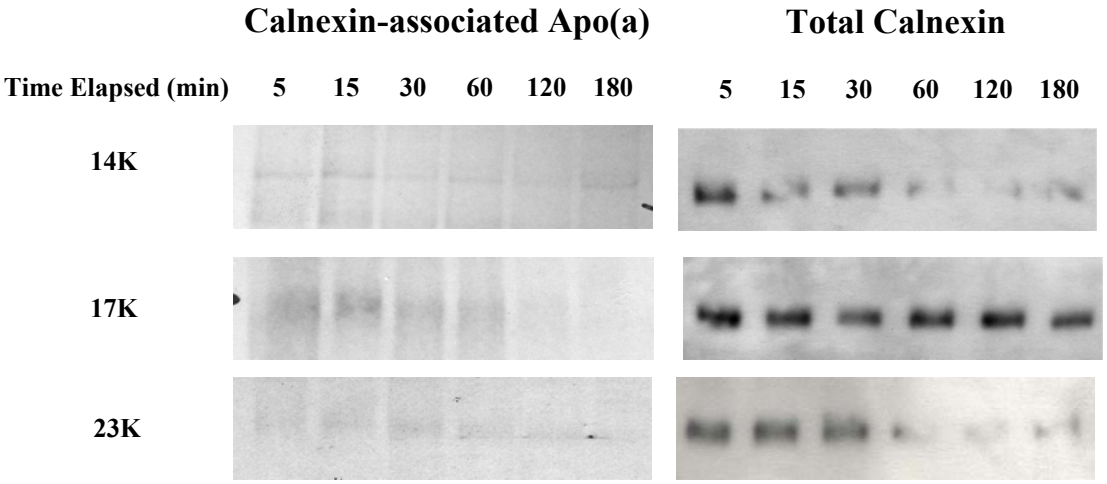

Figure 15: *Intracellular association of apo(a) with Calnexin:* Cells were metabolically labeled as previously described for determining apo(a) secretion from HepG2 cells (see section 3.1.2), with no addition of DTT prior to the chase period. The chase was performed in serum-free medium, and cells were harvested in the presence of 20mM NEM, as modified from a previous protocol (84). An initial IP was performed using an anti-calnexin antibody, followed by a second IP using an antibody specific for apo(a). Samples containing calnexin-associated apo(a) were analyzed by SDS-PAGE using polyacrylamide gels ranging between 6% to 7% polyacrylamide, fixed, amplified, dried, and subsequently exposed to film for 72 hours. Total lysate calnexin content was also determined, as a normalization tool. Lysate samples were analyzed by SDS-PAGE as before, followed by immunoblotting using an anti-calnexin antibody, as described in section 2.9. Gels are representative of duplicate experiments. Our data indicate that the apo(a) species tested interact with calnexin, although a relationship with isoform size could not be determined conclusively.

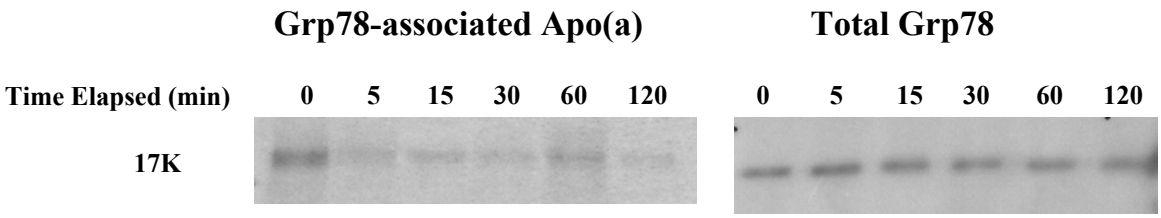

Figure 16: *Intracellular association of apo(a) with Glucose-Regulated Protein 78/Binding Protein (Grp78):* Cells were metabolically labeled as previously described for determining apo(a) secretion from HepG2 cells (see section 3.1.2), with no addition of DTT prior to the chase period. The chase was performed in serum-free medium, and cells were harvested in the presence of 20mM NEM, as modified from a previous protocol (84). An initial IP was performed using an anti-Grp78 antibody, followed by a second IP using an antibody specific for apo(a). Samples containing Grp78-associated apo(a) were analyzed by SDS-PAGE using 6% polyacrylamide gels, fixed, amplified, dried, and subsequently exposed to film for 5 days. Total lysate Grp78 content was also determined, as a normalization tool. Lysate samples were analyzed by SDS-PAGE as before, followed by immunoblotting using an anti-Grp78 antibody, as described in section 2.9. Gels are representative of duplicate experiments. Current experimental data suggest a strong interaction of apo(a) with Grp78 occurs at the onset of the chase period, although continuous association is seen throughout the chase period.

3.4.5 Apo(a) interaction with Grp94

Grp94 is another ER luminal chaperone that provides unfolded proteins an ideal environment to reach proper conformation. Preliminary experimental results seen in *Figure 17* suggest a continuous association between Grp94 and apo(a) during the 120 minute chase period. For both the 14K and 17K isoforms, association with Grp94 seemed to occur in a continuous manner, although interaction appeared to peak at the 15 minute time point.

3.4.6 Apo(a) interaction with EDEM

The ER-Associated Degradation-Enhancing α-Mannosidase-like Protein is a homologue of ER mannosidase I, but lacks the enzymatic activity to process α1, 2-mannose (97). Terminal mannose trimming by α-1, 2-mannosidase of irreversibly misfolded proteins lead to their recognition by EDEM, where they are targeted to the ER-Associated Degradation pathway. *Figure 18* displays the association between EDEM and various apo(a) variants. Apo(a) was seen to interact transiently with EDEM, with larger isoforms (17K and 27K) showing a delayed and more transient interaction with EDEM when compared to the 14K isoform.

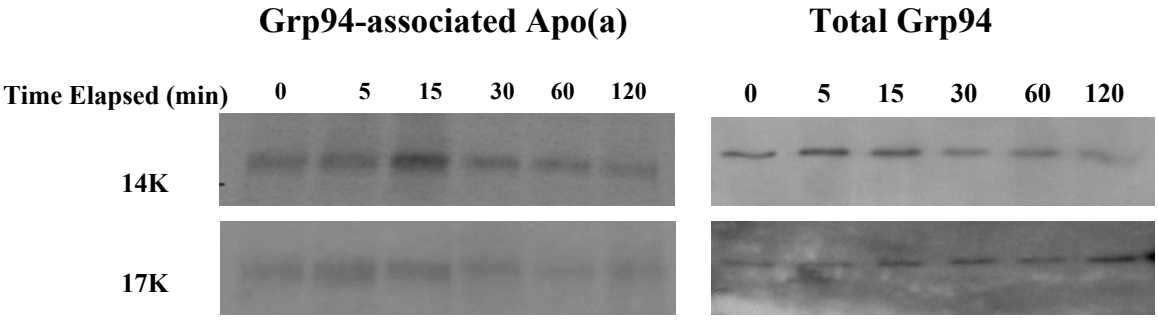

Figure 17: *Intracellular association of apo(a) with Glucose-Regulated Protein 94 (Grp94):* Cells were metabolically labeled as previously described for determining apo(a) secretion from HepG2 cells (see section 3.1.2), with no addition of DTT prior to the chase period. The chase was performed in serum-free medium, and cells were harvested in the presence of 20mM NEM, as modified from a previous protocol (84). An initial IP was performed using an anti-Grp94 antibody, followed by a second IP using an antibody specific for apo(a). Samples containing Grp94-associated apo(a) were analyzed by SDS-PAGE using 6% polyacrylamide gels, fixed, amplified, dried, and subsequently exposed to film for 5 days. Total lysate Grp94 content was also determined, as a normalization tool. Lysate samples were analyzed by SDS-PAGE as before, followed by immunoblotting using an anti-Grp94 antibody, as described in section 2.9. Gels are representative of duplicate experiments. The data clearly demonstrate that apo(a) interacts with Grp94 in a continuous manner.

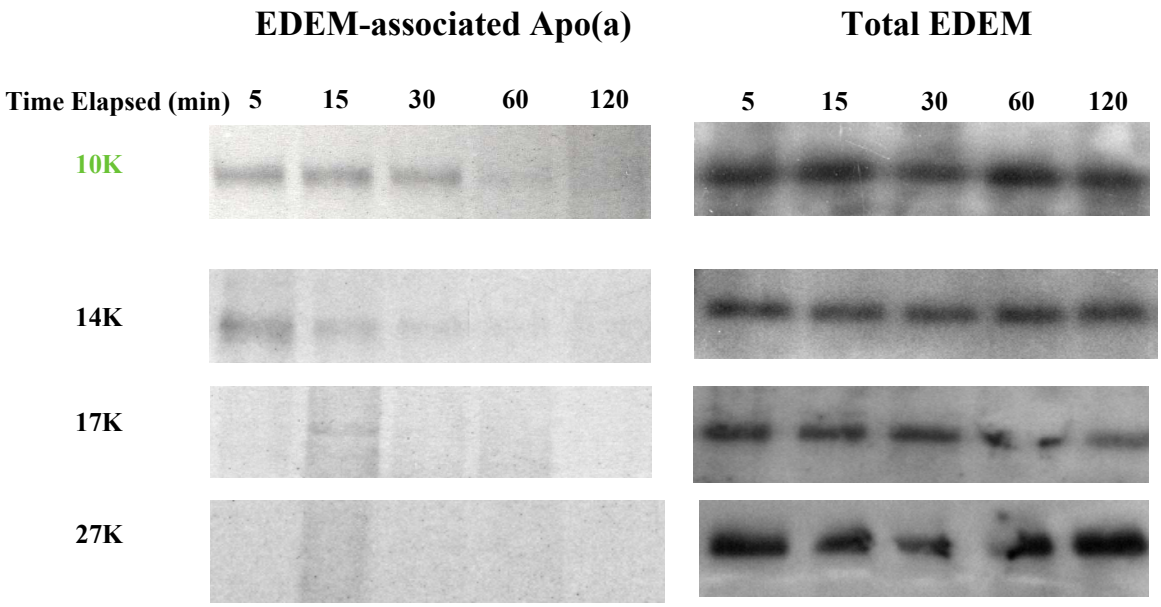

Figure 18: *Intracellular association of apo(a) with ER Degradation-Enhancing α-Mannosidase-like (EDEM):* Cells were metabolically labeled as previously described for determining apo(a) secretion from HepG2 cells (see section 3.1.2), with no addition of DTT prior to the chase period. The chase was performed in serum-free medium, and cells were harvested in the presence of 20mM NEM, as modified from a previous protocol (84). An initial IP was performed using an anti-EDEM antibody, followed by a second IP using an antibody specific for apo(a). Samples containing EDEM-associated apo(a) were analyzed by SDS-PAGE using polyacrylamide gels ranging between 5% to 7% polyacrylamide, fixed, amplified, dried, and subsequently exposed to film for 32 days. Total lysate EDEM content was also determined, as a normalization tool. Lysate samples were analyzed by SDS-PAGE as before, followed by immunoblotting using an anti-EDEM antibody, as described in section 2.9. Gels are representative of duplicate experiments. Taken together, the data suggest that the interaction of 17K and 27K apo(a) with EDEM is delayed when compared to that of the 10K and 14K variants.

3.5 Apolipoprotein(a) Intracellular Degradation

Previous experiments have proposed that, due to the complex post-translational modification of apo(a) which increases with larger size, a greater portion of the larger isoforms remain incompletely processed, and are thus shuttled to protein degradation pathways (28, 33, 104). We have attempted to elucidate the role of proteasomal degradation in HepG2 cells expressing four apo(a) isoforms (14K, 17K, 23K, 27K). The Calpain Inhibitor I (ALLN) was utilized to inhibit proteasomal degradation during the chase period. *Figure 19* shows intracellular and secreted apo(a) levels with (Treated) or without (Control) ALLN addition. The amount of intracellular apo(a) in the presence and absence of ALLN produced no discernable pattern between isoforms. The levels of all isoforms in the medium, however, appeared to increase in the presence of ALLN, with the exception of the 2 hour time point for the 14K apo(a) isoform.

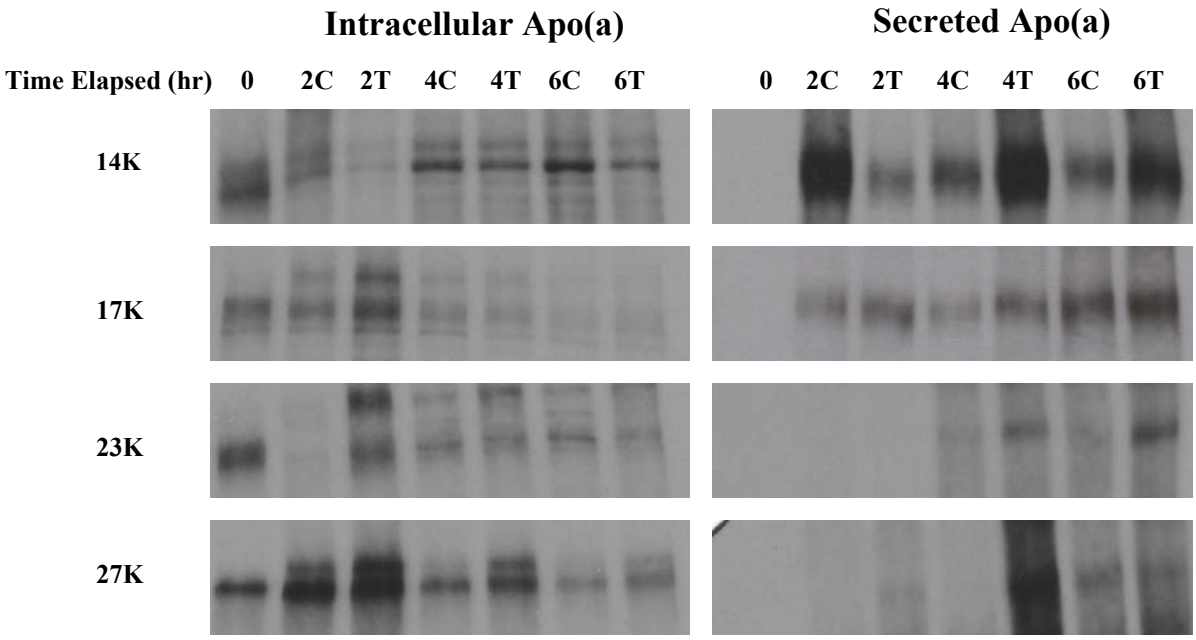

Figure 19*: Inhibition of intracellular apo(a) degradation by the calpain inhibitor ALLN:* Cells were metabolically labeled as before, with no addition of DTT prior to the chase period, and harvested in the presence of 20mM NEM (28). 5μg/mL of the calpain inhibitor I ALLN was added to Treatment plates at the onset of the chase period. In almost all cases, treated (T) samples were correlated with a greater level of secreted apo(a) than control (C) samples.

Chapter 4
Discussion

Lp(a) is synthesized in the liver of humans, old world monkeys, and a homologue is also expressed in the European hedgehog (1, 15). Previous studies on the intracellular processing of apo(a) have been conducted in the hepatocytes of various animals, including baboons, rats, mice and rabbits (8, 41, 1, 105). With the exception of the baboon, none of the other model cell systems used express apo(a) endogenously. For the present study, recombinant apo(a) species stably-expressed in the human hepatoma cell line HepG2 were used to study intracellular apo(a) processing and secretion. The recombinant species used include apo(a) isoforms that are naturally-occurring in the human population as well as a variety of fragments of apo(a) containing specific kringle sequences.

4.1 Analysis of Apolipoprotein(a) Folding

Previous experiments in both primary baboon hepatocytes as well as stably-transfected rat hepatoma (McA-RH7777) and human hepatoma (HepG2) cells have identified two distinct intracellular apo(a) moieties (8, 41, 33). The precursor form of apo(a), termed pr-apo(a), is present at the onset of protein folding, and displays changes as the protein folds that can be observed by non-reduced SDS-PAGE. The heavier, mature apo(a) (m-apo(a)) does not appear until the changes in the mobility of the pr-apo(a) band is complete, indicating that protein folding is complete. Secreted apo(a) was shown to have the same molecular mass as m-apo(a), indicating that the m-apo(a) represents apo(a) that has undergone all major intracellular modifications, including glycosylation modifications (41). No m-apo(a) moiety was seen in our experiments in protein folding, although that may simply be due to the short chase time period of our experiments (84, 85, 68). Previous studies have indicated that, at least in HepG2 cells, the mature

form of apo(a) was only observed after the protein has undergone modifications in the Golgi apparatus (33). At this point, the apo(a) protein would have undergone the majority of its glycosylation modifications, which would cause apo(a) to have an apparent increase in its mass (104), thus appearing as a protein band of lower mobility on an SDS-PAGE gel. It is important to note that previous experiments showing m-apo(a) were conducted over a 4-6 hour chase period, which is much longer than the 12 minute or 2 hour chase period adopted for disulfide bond experiments performed in this study (84, 85, 68). The inability to identify an m-apo(a) moiety may also be partially due to a non-specific protein band present at the same position that the m-apo(a) would have migrated to (Kristina Han, unpublished results).

A small protein with 100 residues may, theoretically, attain roughly 10^{100} conformations from a fully denatured state (114). Most proteins of that size, however, are able to fold in seconds (114). Several folding models exist to explain this Levinthal paradox, all of which result in the formation of a folded conformation that is at the free energy global minimum of the protein (114). The Free-Energy Funnel model involves a thermodynamic view of protein folding (114). Folding commences with the collapse of random coils into a random semi-compact globule (115), which then undergoes several transitory states before the native conformation of the protein is reached. This is a slow process that is accomplished with the aid of chaperones and other ER-resident proteins. This process can be visualized as a Free Energy Funnel, where the top of the funnel represents the most energetic, denatured protein form, and the tip of the funnel represents the native protein conformation with the lowest free energy level. In this model, the narrowing of the funnel, then, represents the decrease in the number of conformational states of lower energy of a protein as its free energy approaches that of the global minimum (114). Investigation into the structural properties of transition states as proteins "slide" down the energy funnel have suggested that larger proteins generally fold in modules (82). Specifically, folding takes place in different

domains of the protein in a way that is largely independent of other domains. The native, most thermodynamically-stable form of the protein is then reached when all interactions within and between domains become locked in their native state (82). Two different types of folding patterns are seen for apo(a) between HEK 293 and HepG2 cells.

4.1.1 Analysis of Apo(a) Folding in HEK 293 Cell

The formation of disulfide bonds in apo(a) in HEK 293 cells occurs in a quick, isoform-dependent manner (*Figure 9*). Larger isoforms appear to delay bond formation until 6-9 minutes into the chase period, whereas the smaller isoforms showed immediate commencement of disulfide bond formation in the form of band shifts after the removal of DTT. The KIV_{5-10} fragment and 6K fragments both showed band mobility shifts between the 0 and 3 minute time points, potentially indicating that the protease domain is not required in apo(a) folding. Our experimental protocol, however, cannot indicate whether the presence of this protease domain significantly delays the folding of apo(a) fragments.

A sequential folding pattern was suggested by Nassir and colleagues (41). In their study, disulfide bond formation in apo(a) was compared between rat hepatoma McA-RH7777 cells expressing 6K and 13K apo(a) variants (41). The 6K variant was completely folded within 30 minutes of the chase period, whereas the 13K isoform showed continual shifts in the apo(a) band until the 90-minute time point. It was concluded that apo(a) folded in a manner dependent on the number of KIV repeats. The smaller variant used in this experiment, however, lacked the KIV_{2-4} domains, and thus is not a physiologically relevant apo(a) isoform. As such, these experiments may not have reflected the pattern of disulfide bond formation in apo(a) folding seen between larger apo(a) isoforms.

The isoform-dependent folding pattern in HEK 293 cells may be in agreement with the results of Nassir and colleagues. As the isoforms used in our study vary only by the number of KIV_2 motifs, folding of this segment may be the rate-determining step in HEK 293 cells. Larger isoforms with more KIV_2 domains, therefore, may require the formation of some, or all, disulfide bonds in previous domains before subsequent folding can occur in the rest of the protein, giving rise to a size-dependent folding mechanism.

4.1.2 Analysis of Apo(a) Folding in HepG2 Cells

The formation of disulfide bonds in apo(a) occurs at a much slower rate in HepG2 cells when compared to HEK 293 cells, and are exponentially slower than other secretory proteins (116). Previous experiments in baboon and rat hepatocytes have, however, shown similar rates of bond formation to those that we have seen in HepG2 cells here (8, 41). Experiments performed by White and colleagues showed that apo(a) in baboon hepatocytes reached maximum band mobility approximately 60 minutes into the chase period (8). The 13K isoform was seen to fold within 90 minutes of the chase period in rat mcA-RH7777 cells in experiments performed by Nassir and colleagues (41). Both the 10K and 14K apo(a) variants studied in our experiments were seen to reach maximum band mobility shift by 60 minutes of chase. Our findings are comparable to apo(a) folding kinetics seen in primary baboon hepatocytes, indicating isoform-independent disulfide bond formations (8). As reported by White and co-workers (8), our data suggests that apo(a) kringles fold simultaneously and independently from each other, and are not affected by the presence or abundance of neighbouring motifs. This is in agreement with the protein folding transition state theory, in that intermediate states are formed due to the independent folding of different domains in the protein (82).

Of the four apo(a) isoforms utilized in the study performed by White and co-workers, the smallest isoform investigated was similar in mass to an apo(a) isoform that contained 43K KIV domains, which is much larger than the mean apo(a) isoform size seen in the population (~25K) (8, 40). Three of the four isoforms were also much larger in size, and not reflective of the apo(a) isoform range present in humans (7, 8). In the folding kinetics study performed by Nassir and others, only the 13K apo(a) isoform was of physiological relevance (41). A difference can be seen in our experimental data when comparing the 6K and 14K apo(a) variants, concurrent with the findings of Nassir and coworkers. Our present experiment was able to study the disulfide bond formation of apo(a) in stably transformed human hepatocarcinoma cells expressing isoforms that span more than 60% of the naturally-occurring apo(a) range, and thus was able to provide a more complete understanding of apo(a) folding patterns in humans.

Our experimental design, however, does not allow us to distinguish between different bond permutations as apo(a) undergoes transitory folding states. Due to this limitation, disulfide bond isomerizations that aid in the protein reaching its final conformation, but do not change its compactness, would not be visible in the non-reduced gels. Therefore, it is very probable that the apo(a) conformation reached at the 60-minute time point in HepG2 cells is not the final conformation of the glycoprotein, but rather a low-energy transition state. Based on the isoform-dependent ER-retention time seen in baboon hepatocytes, White and co-workers have suggested a cycle of unfolding and refolding that occurs after the first 60 minutes of apo(a) folding that is not distinguishable on non-reducing SDS-PAGE gels (8). The existence of such disulfide bond exchanges is further supported by clear interactions of apo(a) with PDI and Erp57 after the first hour of folding (*Figures 13 and 14*; see sections 3.4.1 and 3.4.2, respectively). Apo(a) is also a highly glycosylated protein species, and previous experiments have indicated proper glycosylation to be critical in the secretion of apo(a) from the ER (25, 84, 85). Subsequent

modifications of apo(a) after disulfide bond formation, therefore, may be a greater influence in determining the rate at which apo(a) reaches a native conformation than that of disulfide bond formation.

Should apo(a) folding proceed independently of the number of kringle motifs present in the protein, apo(a) fragments would be expected to fold in a manner similar to isoforms. Closer examination of the folding of apo(a) fragments in HepG2 cells, however, reveals some size-dependency. The concatomer of three KIV_2 motifs takes less than 5 minutes to fold, whereas the 6K fragment shows changes in mobility indicative of folding up to the 30 minute time point. The 10K fragment, containing all kringle motifs in a single copy, folds in a manner similar to the larger, physiologically relevant isoforms. Based on these observations, it may be possible that apo(a) folds in both a simultaneous and sequential manner. In this case, all kringle domains form disulfide bonds simultaneously, regardless of the number of copies present. This, in turn, would gives rise to the observation of a size-independent folding pattern for apo(a) isoforms and the 10K fragment, where all domains are present in HepG2 cells. At the same time, the interaction between kringle domains required for apo(a) to reach a fully folded conformation occurs in a sequential manner, with domains present later in the sequence requiring earlier domains to reach a specific folding or glycosylation state before they are able to commence interaction with the rest of the protein. Smaller apo(a) fragments are missing several KIV domains in their structure, and thus would not require as long to fold as constructs containing all domains. These would then reach a folded state much faster than larger isoforms, giving rise to a size-dependent folding pattern. Further experimentation should be performed utilizing experimental designs that can distinguish between different folded and glycosylated states of apo(a). Investigation of apo(a) deletion mutants lacking different kringle domains, especially KIV_2, may also be useful.

4.2 Apolipoprotein(a) Secretion

Isoform size-dependent apo(a) secretion was seen in both HEK 293 and HepG2 cells, which is consistent with previous reports (33, 104). For both cell lines, larger isoforms appeared much later in the conditioned medium of pulse-labeled cells than smaller isoforms. In HEK 293 cells, the 12-minute chase period was not long enough to observe the appearance of all apo(a) isoforms. It is apparent, however, that time points at which non-reduced apo(a) bands cease to change in mobility correspond well to the appearance of apo(a) in the medium (*Figure 9* and *Figure 11*), suggesting that rapid post-translational modification steps are involved between folding and secretion of apo(a) in HEK 293 cells. Due to the slow folding time of apo(a) in HepG2 cells, the secretion chase period was extended to 6 hours after the commencement of folding. With no addition of DTT at the start of the chase period to denature folded proteins, the 0 time point in the secretion experiments (*Figure 12*) is equal to the 60 minute time point in the folding experiments (*Figure 10*). Larger isoforms took much longer to appear in the medium (compare 10K-30 minutes, 14K-60 minutes, and 23K-120 minutes).

Larger apo(a) isoforms have been shown to secrete at a later time than smaller isoforms in primary baboon hepatocytes, partially due to the longer ER-retention time of the larger isoforms seen in experiments performed by White and coworkers (36). In their study, Brunner and others determined that a 22K apo(a) isoform was also secreted at a slower rate than an 11K apo(a) variant, both stably expressed in HepG2 cells (33). The apo(a) secretion kinetics seen in our study displayed a similar isoform size dependency as was seen previously, further confirming these previous findings with the greater range of apo(a) isoform sizes studied here (*Figure 12*) (33, 36).

Our methodology, once again, does not allow for quantification of the amount of apo(a) secreted into the conditioned medium as a function of time. As such, our data cannot be analyzed to determine differences in the efficiency of apo(a) secretion with respect to isoform size. We have, however, shown qualitative evidence that the appearance of apo(a) in the cellular medium occurs at a later time point for larger isoforms. Further investigation into apo(a) secretion in a quantitative context should include at least two other components. A purified, radiolabelled standard of known apo(a) concentration corresponding in size to the apo(a) variant should be run alongside the experimental samples on SDS-PAGE gels to quantify the total amount of apo(a) present in each sample. The total amount of apo(a) present in the medium, then, should be normalized to the total amount of apo(a) present in the cell lysate, determined by a quantitative ELISA method (117), in order to determine the efficiency of apo(a) secretion with respect to isoform size.

We have shown that apo(a) folding in HepG2 cells occur independent of isoform size (*Figure 10*). Previous and current experimental results from secretion studies, however, indicate that apo(a) appearance in the conditioned medium occurs in an isoform size-dependent manner (*Figure 12*) (33, 36). Taken together, these data provide strong evidence that the processes involved in the regulation of secretion of apo(a) from cells are influenced by its isoform size. This, in turn, affects the rate at which differently-sized isoforms are secreted from cells, and likely underscores the inverse correlation between isoform size and the amount of apo(a) secreted by the cells. Due to the differences in folding patterns between HEK 293 and HepG2 cells, and that HepG2 cells represent the more relevant cell type, further experiments were performed exclusively using HepG2 cells.

4.3 Apolipoprotein(a) Intracellular Modifications

Previous research have indicated that the isoform-size dependency in apo(a) secretion from HepG2 cells were partially due to a longer retention time of larger isoforms in the ER (33), suggesting an isoform size-dependent interaction of apo(a) with ER-resident enzymes. Several ER-resident proteins have been characterized as players in the protein folding and glycosylation modification pathways. The multimeric complex involving Grp78, Grp94, and PDI has been shown to interact with nascent polypeptides to aid in protein folding and other post-translational modifications (87). Furthermore, as a glycoprotein, apo(a) also interacts with lectins such as Cnx and Crt, as well as the glycoprotein-specific isomerase Erp57, for proper folding and trimming of glycans before the protein can be transported out of the ER (106). Our goal for these studies was to study the intracellular association of differently-sized apo(a) isoforms with these chaperones and folding enzymes, as well as with the ER degradation-enhancing α-mannosidase-like enzyme (EDEM), which shuttle irreversibly-misfolded proteins to the intracellular degradation pathway.

4.3.1 Apo(a) Interaction with PDI and Erp57

Apo(a) association with the thiol-isomerase PDI appeared to be transient in nature (*Figure 13*). Intriguingly, smaller variants (10K, 14K) appeared to associate with PDI for a prolonged time, whereas larger isoforms appeared to dissociate from the catalyst 30 minutes into the chase period. Previous experiments performed by Nassir and others showed a 13K isoform of apo(a) transiently interacting with PDI in rat hepatoma McA-RH777 cells, with dissociation occurring approximately 60 minutes into the chase period (41). One explanation for the prolonged association of PDI with smaller isoforms may be the increased shuffling of larger, misfolded apo(a) moieties directly into the ERAD pathway. Smaller isoforms may be more efficient in reaching the Cnx/Crt cycle in a relatively folded state, reaching their native form in

the cycle, and have a greater probability of being secreted, resulting in higher secretion efficiency than larger isoforms. More experiments, possibly with a different PDI antibody to determine the validity of current trends, must be performed to support the current hypothesis.

Erp57 is a glycoprotein-specific isomerase, aiding in the folding and refolding of newly synthesized glycoproteins. A strong initial association between apo(a) and Erp57 was seen, followed by a quick partial dissociation (*Figure 14*). A basal level of association between apo(a) and Erp57, however, was maintained for a prolonged period (23K apo(a) in *Figure 14*), and this residual association is presumably due to the interaction between apo(a) and the Cnx/Erp57 complex as the glycoprotein enters the Cnx/Crt cycle (91). Further experiments with a wider range of apo(a) isoforms would shed more light on the association kinetics between Erp57 and apo(a). The association of apo(a) with the two isomerases also provides support for the hypothesis that apo(a) has not yet reached a fully folded form 60 minutes after folding commences.

4.3.2 Apo(a) Association with Calnexin

The Cnx/Crt cycle ensures that newly-synthesized glycoproteins are properly folded and glycosylated, and is the last regulatory check point for glycoproteins before they are secreted from the ER (91). Previous studies have shown that the glycoprotein apo(a) is retained in the ER in an isoform-dependent manner, and the rate at which apo(a) is secreted out of the ER directly influences apo(a) secretion efficiency (36, 85, 84). This, then, suggests a possible isoform-dependent interaction between apo(a) and the Cnx/Crt cycle. Interaction between apo(a) and calnexin has been shown in stably transformed rat hepatoma McA-RH7777 (41) and mice hepatocytes (84) cells expressing 13K and 17K apo(a) isoforms, respectively. In both cell lines, apo(a) appeared to sustain significant interaction with calnexin within the first 30-60 minutes of

the chase period in a pulse-chase experiment, and decreased to a baseline interaction level at the 120 minute time point for the 17K isoform (41, 84).

Very little apo(a) interaction with the lectin Cnx was detected in HepG2 cells over a period of 180 minutes (*Figure 15*). Current experimental results have shown that all isoforms interact with the lectin, however there is no clear trend between isoform size and association kinetics. The 17K isoform in HepG2 appeared to interact with calnexin in a similar manner as the 17K apo(a) isoform expressed in mice hepatocytes (84). More experimentation must be conducted with other isoforms, utilizing another protocol with superior detection of Cnx-apo(a) association. Association with the other lectin involved in the Cnx/Crt cycle, calreticulin, has also been previously shown with stably transformed mice hepatocytes expressing the 17K apo(a) isoform, and show an association kinetic similar to that of apo(a)-calnexin interaction, albeit at a weaker level of interaction (84). In rat hepatoma, calreticulin was also shown to interact in a continuous manner with the 13K apo(a) isoform throughout the 180 minute chase period (41). Therefore, investigation into apo(a) association with the other members of the Cnx/Crt cycle, including Crt and UGGT (91), may provide a better understanding of the interaction between apo(a) and the glycosylation checkpoint with respect to apo(a) size.

4.3.3 Apo(a) Association with Grp78 and Grp94

Grp78 and Grp94 are chaperone proteins that interact with most proteins that fold in the ER (86). In rat hepatoma cells, a 13K apo(a) isoform was shown to interact strongly with Grp78 during the first 60 minutes of the chase period in a pulse-chase experiment (41). Preliminary results showing the interaction between Grp78 and a 17K apo(a) isoform, and Grp94 with the 14K and 17K apo(a) isoforms, indicated that apo(a) associates with both chaperones in a continuous manner, increasing in association early on during the 120 minute chase period

(*Figures 16-17*). Initial interaction between apo(a) and Grp78 mirrored that of apo(a)-Erp57 interactions (*Figures 14 and 16*). Grp78 and Erp57 are both folding initiators, interacting with the nascent polypeptide chain first before passing the interaction along to other enzymes, and as such, would be expected to interact in a similar manner with newly synthesized apo(a) (91, 93). Apo(a) association with Grp94 appeared to be size-independent, as both 14K and 17K apo(a) associated with Grp94 continuously at approximately the same level, with a single peak at the 15 minute time point (*Figure 17*). Grp94 is proposed to associate with polypeptides after they have dissociated from Grp78, as was seen here (*Figures 16-17*) (87). Given that Grp94 is one of the most abundant ER chaperone enzymes present in the ER (118), the low detection in total Grp94 in our samples suggests a low-efficiency Grp94 capture antibody (*Figure 17,* right). An alternative Grp94 detection antibody may provide a clearer description of the apo(a)-Grp94 interaction as a function of isoform size. The continuous manner with which apo(a) associates with both Grp78 and Grp94 may also indicate a pool of perpetually misfolded apo(a) species in the ER lumen. More apo(a) isoforms must be examined for their interaction with these chaperone proteins to validate our current findings.

4.3.4 Apo(a) Association with EDEM

EDEM shuttles misfolded, mannose-trimmed glycoproteins from the Cnx/Crt cycle to the ERAD pathway, and thus would be expected to associate with apo(a) later in the chase period. In our study, however apo(a) association with EDEM appeared to occur at or shortly after apo(a) reaches a stable transition state which may be explained via an indirect association with Cnx, as EDEM colocalizes with Cnx on the ER membrane (45) (*Figure 18*). This association was also seen to be somewhat inversely related to apo(a) isoform size, with smaller isoforms having a stronger, longer association with EDEM than larger isoforms. Investigating the interaction

between apo(a) and α 1,2-mannosidase, the enzyme that catalyses the removal of a terminal mannose from the glycan chain to identify a protein as an EDEM target (97), may provide a better understanding of the role of ERAD in intracellular apo(a) modifications.

4.3.5 Limitations of the Studies and Future Directions

Our data cannot provide conclusive evidence to support the hypothesis that apo(a) isoform size plays a specific role in intracellular processing. Further experimentation should be conducted on different apo(a) isoforms, along with additional investigation into the interaction between apo(a) and other proteins and complexes such as Glucosidases I and II, UGGT, and the ER-Golgi intermediate compartment (ERGIC), in order to provide a more thorough understanding of the dynamics between apo(a) isoform size and intracellular processing. Low detection levels, possibly caused by poor antibody recognition also appear to be a hindrance in studying apo(a) interactions with several ER-resident enzymes. As such, it may be useful to cross-link apo(a) with its associated proteins during the primary immunoprecipitation step to preserve the interactions between the two components throughout the immunoprecipitation process. Dimethyl 3, 3'-dithiobispropionimidate (DTBP) and the Lomant's reagent dithiobis(succinimidyl propionate) (DSB) have both been shown to function as thiol-reducible chemical cross-linkers in rat hepatocyte lysates (119). Addition of these cross-linkers during the collection steps may increase the amount of apo(a) that appears on the SDS-PAGE gels, providing clearer association patterns between apo(a) and the ER-resident enzymes.

The ER-resident enzymes studied here are involved in the modification of many other proteins, and play many roles in the regulation of ER and protein folding homeostasis (93). Any attempts at regulating apo(a) secretion levels that target one of these enzymes will inevitably lead to the disruption of several other vital cellular procedures (87). Therefore, these enzymes would

not be ideal as targets for decreasing apo(a) secretion from hepatocytes. For this application, other intracellular processes must be explored in order to provide better alternatives in regulating the rate and extent of apo(a) secretion.

4.4 Intracellular Degradation of Apolipoprotein(a)

Previous experiments have provided strong evidence that the efficiency of apo(a) secretion is partially due to the extent of intracellular degradation that occurs as apo(a) travels from the ER to the plasma membrane (24, 28, 84). Inhibition of both protease activity ((21), as well as apo(a) ER secretion (84), were shown increase the secretory level of larger apo(a) isoforms and increase intracellular pr-apo(a) levels (28). This increase in intracellular apo(a) level was also seen with inhibitors that compromise the retrotranslocation of apo(a) into the cytosol, a crucial step in the process of cytoplasmic degradation (24) . Finally, the precursor form of apo(a) has been shown to interact with ubiquitin (28), indicating that apo(a) is degraded through a proteasome-mediated degradation pathway.

Proteasomal degradation is the most well-characterized intracellular degradation process, and is also associated with ERAD (102). Preliminary results suggest that, in general, inhibition of proteasomal degradation increased the level of secreted apo(a) from HepG2 cells (*Figure 19)*. This implies a major role of proteasomal degradation in the secretion efficiency of apo(a). However, no observable trend was seen with intracellular apo(a) levels in the presence and absence of ALLN, as was seen in previous experiments (28). Increasing intracellular degradation of apo(a), especially of small apo(a) isoforms, may be one form of regulating apo(a) secretion, and subsequently plasma Lp(a) levels. As such, more experimentation must be performed to determine the effect of proteasomal degradation on intracellular apo(a) levels. The relationship between the secreted levels of differently-sized apo(a) and the presence and abundance of

intracellular precursor and mature apo(a) should also be explored. It may be worthwhile to consider exploring the temporal and spatial dynamics of intracellular apo(a) processes with respect to isoform size using a fluorescence label. This would provide a basic understanding of the apo(a) population distribution within the cell, as well as the percentage of synthesized apo(a) that is targeted to either the secretory or degradation pathways.

Chapter 5

Conclusion

The vast number of clinical reports has painted Lp(a) as a complex lipoprotein dynamic in its function and plasma concentrations. A strong genetic control, coupled with a synthesis-dependent plasma concentration places value on the study of the two components of Lp(a), apoB-100 and apo(a), and their respective syntheses and secretion (4, 6, 30, 32, 37, 120). While apoB-100-LDL has been thoroughly studied due to the well-established role of elevated plasma LDL concentrations in CHD, the unusual species distribution of apo(a) has severely limited studies performed on this Lp(a) component. As such, there is still much debate with respect to fundamental questions about Lp(a), including regulation of its synthesis and catabolism, as well as its role in human physiology. The present study represents an initial investigation of the processes involved in the intracellular processing and secretion of apo(a) from HepG2 cells.

Comparison between HEK 293 and HepG2 cell lines revealed marked differences in apo(a) folding pattern. The formation of disulfide bonds in HEK 293 cells displayed isoform size-dependency, accompanied by rapid intracellular maturation and secretion of apo(a) from these cells. In contrast, we observed that in HepG2 cells, disulfide bonds formed in a size-independent manner, even though secretion from both cell lines appeared to be isoform size-dependent. This size-independent apo(a) folding pattern in HepG2 cells is consistent with previous experimental findings for the study of apo(a) folding in baboon hepatocytes (8), and provides support for the validity of other experiments performed in these cells (85, 84). Based on experimental results, we propose that apo(a) may fold in both a simultaneous and sequential manner. Motifs of identical amino acid sequences, such as the KIV_2 domains, may form disulfide bonds within kringles simultaneously regardless of the number of copies present. At the same

time, different kringles may interact with each other sequentially, with domains encoded later in the sequence requiring the formation of a specific conformation state in previous domains before they are able to participate in the inter-kringle interactions. Further experimentation should be conducted with apo(a) deletion mutants lacking specific kringle motifs to investigate the validity of our proposed apo(a) folding mechanism in HepG2 cells.

Preliminary experiments revealed that several ER-resident enzymes interact with apo(a) in a manner characteristic of the intracellular processing of glycoproteins in mammalian cells. Interaction of all apo(a) isoforms with chaperone proteins and isomerases showed that the previously assumed folding "completion" (as indicated by a lack of further changes in mobility in non-reduced apo(a) band shift) signified that the glycoprotein had only reached a low-energy transition state, and was still undergoing disulfide bond exchange within the protein itself. Apo(a) was shown to interact transiently with Erp57, and EDEM, and continuously with Grp78 and Grp94. Both PDI and calnexin appeared to associate continuously with the 14K apo(a) isoform, but were seen to interact transiently with larger isoforms (>17K). Further experimentation with other apo(a) isoforms must be conducted to confirm and expand current trends. Interactions of different apo(a) isoforms with other ER-resident proteins, such as α 1,2-mannosidase and UGGT, should also be investigated to enhance our understanding of the processes and enzymes involved in apo(a) intracellular maturation with respect to apo(a) isoform size.

A prominent increase in secreted apo(a) of all isoform sizes was seen when cytoplasmic proteasomal degradation was inhibited, indicating a major role for ERAD degradation in apo(a) secretion efficiency. Preliminary results did not show a discernable trend in intracellular apo(a) content in the presence of ALLN, although previous research have shown increases in the precursor form of apo(a) in the presence of protease inhibitors in primary mice and baboon

hepatocytes (24, 28). Experiments must be repeated to confirm our results obtained in HepG2 cells. Since the retrotranslocation of misfolded proteins from the ER to the cytosol is crucial in the process of cytoplasmic degradation, examining the role of ERAD-associated translocon activity with respect to apo(a) size may also be useful in determining the influence of intracellular degradation on apo(a) secretion efficiency as a function of isoform size (28).

We have, in this study, provided an initial investigation into the intracellular processes involved in apo(a) synthesis and secretion in HepG2 cells. Apo(a) appears to fold in an isoform-dependent manner in HEK 293 cells, but show isoform size-independent folding kinetics in HepG2 cells. Secretion of apo(a) from both cell lines appears to be isoform size-dependent. Apo(a) appears to associate with ER-resident enzymes that are commonly involved in intracellular maturations of glycoproteins, and all isoforms undergo proteasome-mediated degradation prior to secretion. Future studies must be carried out to expand our initial findings on the apo(a) interaction with ER-resident enzymes with respect to isoform size, confirm hypotheses proposed from preliminary experimental results, and explore other intracellular processes in apo(a) synthesis and secretion with the goal of understanding the molecular basis of apo(a) processing and secretion as a function of isoform size.

References

1. Makino, K., and A. M. Scanu. 1991. Lipoprotein(a): nonhuman primate models. *Lipids* 26: 679-683.

2. Laplaud, P., L. Beaubatie, S. Rall, G. Luc, and M. Saboureau. 1988. Lipoprotein[a] is the major apoB-containing lipoprotein in the plasma of a hibernator, the hedgehog (Erinaceus europaeus). *J. Lipid Res.* 29: 1157-1170.

3. Koschinsky, M. L. 2005. Lipoprotein(a) and atherosclerosis: new perspectives on the mechanism of action of an enigmatic lipoprotein. *Curr Atheroscler Rep* 7: 389-395.

4. Koschinsky, M. L. 2006. Novel insights into Lp(a) physiology and pathogenicity: more questions than answers? *Cardiovasc Hematol Disord Drug Targets* 6: 267-278.

5. McLean, J. W., J. E. Tomlinson, W. J. Kuang, D. L. Eaton, E. Y. Chen, G. M. Fless, A. M. Scanu, and R. M. Lawn. 1987. cDNA sequence of human apolipoprotein(a) is homologous to plasminogen. *Nature* 330: 132-137.

6. Boerwinkle, E., C. C. Leffert, J. Lin, C. Lackner, G. Chiesa, and H. H. Hobbs. 1992. Apolipoprotein(a) gene accounts for greater than 90% of the variation in plasma lipoprotein(a) concentrations. *J Clin Invest.* 90: 52–60.

7. Marcovina, S. M., J. J. Albers, E. Wijsman, Z. Zhang, N. H. Chapman, and H. Kennedy. 1996. Differences in Lp[a] concentrations and apo[a] polymorphs between black and white Americans. *J. Lipid Res* 37: 2569-2585.

8. White, A. L., B. Guerra, and R. E. Lanford. 1997. Influence of allelic variation on apolipoprotein(a) folding in the endoplasmic reticulum. *J. Biol. Chem* 272: 5048-5055.

9. Sandholzer, C., E. Boerwinkle, N. Saha, M. C. Tong, and G. Utermann. 1992. Apolipoprotein(a) phenotypes, Lp(a) concentration and plasma lipid levels in relation to coronary heart disease in a Chinese population: evidence for the role of the apo(a) gene in coronary heart disease. *J. Clin. Invest* 89: 1040-1046.

10. Koschinsky, M. L., G. P. Côté, B. Gabel, and Y. Y. van der Hoek. 1993. Identification of the cysteine residue in apolipoprotein(a) that mediates extracellular coupling with apolipoprotein B-100. *J. Biol. Chem* 268: 19819-19825.

11. Brunner, C., H. G. Kraft, G. Utermann, and H. J. Müller. 1993. Cys4057 of apolipoprotein(a) is essential for lipoprotein(a) assembly. *Proc. Natl. Acad. Sci. U.S.A* 90: 11643-11647.

12. Anglés-Cano, E., and G. Rojas. 2002. Apolipoprotein(a): structure-function relationship at the lysine-binding site and plasminogen activator cleavage site. *Biol. Chem* 383: 93-99.

13. van der Hoek, Y. Y., M. E. Wittekoek, U. Beisiegel, J. J. Kastelein, and M. L. Koschinsky. 1993. The apolipoprotein(a) kringle IV repeats which differ from the major repeat kringle are present in variably-sized isoforms. *Hum. Mol. Genet* 2: 361-366.

14. Marcovina, S. M., H. H. Hobbs, and J. J. Albers. 1996. Relation between number of apolipoprotein(a) kringle 4 repeats and mobility of isoforms in agarose gel: basis for a standardized isoform nomenclature. *Clin. Chem* 42: 436-439.

15. Hobbs, H. H., and A. L. White. 1999. Lipoprotein(a): intrigues and insights. *Curr. Opin. Lipidol* 10: 225-236.

16. Koschinsky, M. L., U. Beisiegel, D. Henne-Bruns, D. L. Eaton, and R. M. Lawn. 1990. Apolipoprotein(a) size heterogeneity is related to variable number of repeat sequences in its mRNA. *Biochemistry* 29: 640-644.

17. Lackner, C., J. C. Cohen, and H. H. Hobbs. 1993. Molecular definition of the extreme size polymorphism in apolipoprotein(a). *Hum. Mol. Genet* 2: 933-940.

18. Becker, L., P. M. Cook, T. G. Wright, and M. L. Koschinsky. 2004. Quantitative evaluation of the contribution of weak lysine-binding sites present within apolipoprotein(a) kringle IV types 6-8 to lipoprotein(a) assembly. *J. Biol. Chem* 279: 2679-2688.

19. Becker, L., R. S. McLeod, S. M. Marcovina, Z. Yao, and M. L. Koschinsky. 2001. Identification of a critical lysine residue in apolipoprotein B-100 that mediates noncovalent interaction with apolipoprotein(a). *J. Biol. Chem* 276: 36155-36162.

20. Xu, S. 1998. Apolipoprotein(a) binds to low-density lipoprotein at two distant sites in lipoprotein(a). *Biochemistry* 37: 9284-9294.

21. Gabel, B. R., and M. I. Koschinsky. 1995. Analysis of the proteolytic activity of a recombinant form of apolipoprotein(a). *Biochemistry* 34: 15777-15784.

22. Ernst, E. 1994. Fibrinogen: an important risk factor for atherothrombotic diseases. *Ann. Med* 26: 15-22.

23. Hancock, M. A., M. B. Boffa, S. M. Marcovina, M. E. Nesheim, and M. L. Koschinsky. 2003. Inhibition of plasminogen activation by lipoprotein(a): critical domains in apolipoprotein(a) and mechanism of inhibition on fibrin and degraded fibrin surfaces. *J. Biol. Chem* 278: 23260-23269.

24. Wang, J., and A. L. White. 1999. 6-Aminohexanoic acid as a chemical chaperone for apolipoprotein(a). *J. Biol. Chem* 274: 12883-12889.

25. Bonen, D. K., F. Nassir, A. M. Hausman, and N. O. Davidson. 1998. Inhibition of N-linked glycosylation results in retention of intracellular apo[a] in hepatoma cells, although nonglycosylated and immature forms of apolipoprotein[a] are competent to associate with apolipoprotein B-100 in vitro. *J. Lipid Res* 39: 1629-1640.

26. Utermann, G., H. J. Menzel, H. G. Kraft, H. C. Duba, H. G. Kemmler, and C. Seitz. 1987. Lp(a) glycoprotein phenotypes. Inheritance and relation to Lp(a)-lipoprotein concentrations in plasma. *J. Clin. Invest* 80: 458-465.

27. Schmidt, K., H. G. Kraft, W. Parson, and G. Utermann. 2006. Genetics of the Lp(a)/apo(a) system in an autochthonous Black African population from the Gabon. *Eur. J. Hum. Genet* 14: 190-201.

28. White, A. L., B. Guerra, J. Wang, and R. E. Lanford. 1999. Presecretory degradation of apolipoprotein [a] is mediated by the proteasome pathway. *J. Lipid Res* 40: 275-286.

29. Krempler, F., G. M. Kostner, K. Bolzano, and F. Sandhofer. 1980. Turnover of lipoprotein (a) in man. *J. Clin. Invest* 65: 1483-1490.

30. Marcovina, S. M., M. L. Koschinsky, J. J. Albers, and S. Skarlatos. 2003. Report of the National Heart, Lung, and Blood Institute Workshop on Lipoprotein(a) and Cardiovascular Disease: recent advances and future directions. *Clin. Chem* 49: 1785-1796.

31. Kostner, K. M., and G. M. Kostner. 2004. Factors affecting plasma lipoprotein(a) levels: role of hormones and other nongenetic factors. *Semin Vasc Med* 4: 211-214.

32. Rader, D. J., W. Cain, K. Ikewaki, G. Talley, L. A. Zech, D. Usher, and H. B. Brewer. 1994. The inverse association of plasma lipoprotein(a) concentrations with apolipoprotein(a) isoform size is not due to differences in Lp(a) catabolism but to differences in production rate. *J. Clin. Invest* 93: 2758-2763.

33. Brunner, C., E. M. Lobentanz, A. Pethö-Schramm, A. Ernst, C. Kang, H. Dieplinger, H. J. Müller, and G. Utermann. 1996. The number of identical kringle IV repeats in apolipoprotein(a) affects its processing and secretion by HepG2 cells. *J. Biol. Chem* 271: 32403-32410.

34. Edjème-Aké, A., R. Garnotel, S. Vallée-Polneau, E. Anglés-Cano, D. Monnet, and P. Gillery. 2008. Relationship between apo(a) length polymorphism and lipoprotein(a) concentration in healthy Ivorian subjects with single or double apo(a) isoforms. *Clin. Biochem* 41: 1039-1043.

35. Tsimikas, S., P. Clopton, E. S. Brilakis, S. M. Marcovina, A. Khera, E. R. Miller, J. A. de Lemos, and J. L. Witztum. 2009. Relationship of oxidized phospholipids on apolipoprotein B-100 particles to race/ethnicity, apolipoprotein(a) isoform size, and cardiovascular risk factors: results from the Dallas Heart Study. *Circulation* 119: 1711-1719.

36. White, A. L., J. E. Hixson, D. L. Rainwater, and R. E. Lanford. 1994. Molecular basis for "null" lipoprotein(a) phenotypes and the influence of apolipoprotein(a) size on plasma lipoprotein(a) level in the baboon. *J. Biol. Chem* 269: 9060-9066.

37. Becker, L., P. M. Cook, and M. L. Koschinsky. 2004. Identification of sequences in apolipoprotein(a) that maintain its closed conformation: a novel role for apo(a) isoform size in determining the efficiency of covalent Lp(a) formation. *Biochemistry* 43: 9978-9988.

38. Becker, L., B. A. Webb, S. Chitayat, M. E. Nesheim, and M. L. Koschinsky. 2003. A ligand-induced conformational change in apolipoprotein(a) enhances covalent Lp(a) formation. *J. Biol. Chem* 278: 14074-14081.

39. Marcovina, S. M., and M. L. Koschinsky. 2002. A critical evaluation of the role of Lp(a) in cardiovascular disease: can Lp(a) be useful in risk assessment? *Semin Vasc Med* 2: 335-344.

40. Rubin, J., F. Paultre, C. H. Tuck, S. Holleran, R. G. Reed, T. A. Pearson, C. M. Thomas, R. Ramakrishnan, and L. Berglund. 2002. Apolipoprotein [a] genotype influences isoform dominance pattern differently in African Americans and Caucasians. *J. Lipid Res* 43: 234-244.

41. Nassir, F., Y. Xie, and N. O. Davidson. 2003. Apolipoprotein[a] secretion from hepatoma cells is regulated in a size-dependent manner by alterations in disulfide bond formation. *J. Lipid Res* 44: 816-827.

42. Kang, S., and R. A. Davis. 2000. Cholesterol and hepatic lipoprotein assembly and secretion. *Biochim. Biophys. Acta* 1529: 223-230.

43. Ni, M., and A. S. Lee. 2007. ER chaperones in mammalian development and human diseases. *FEBS Lett* 581: 3641-3651.

44. Qiu, W., R. Kohen-Avramoglu, F. Rashid-Kolvear, C. S. Au, T. M. Chong, G. F. Lewis, D. K. Y. Trinh, R. C. Austin, R. Urade, and K. Adeli. 2004. Overexpression of the endoplasmic reticulum 60 protein ER-60 downregulates apoB100 secretion by inducing its intracellular degradation via a nonproteasomal pathway: evidence for an ER-60-mediated and pCMB-sensitive intracellular degradative pathway. *Biochemistry* 43: 4819-4831.

45. Helenius, A., and M. Aebi. 2004. Roles of N-linked glycans in the endoplasmic reticulum. *Annu. Rev. Biochem* 73: 1019-1049.

46. Gazzaruso, C., R. Bruno, A. Pujia, E. De Amici, P. Fratino, S. B. Solerte, and A. Garzaniti. 2006. Lipoprotein(a), apolipoprotein(a) polymorphism and coronary atherosclerosis severity in type 2 diabetic patients. *Int. J. Cardiol* 108: 354-358.

47. Danesh, J., R. Collins, and R. Peto. 2000. Lipoprotein(a) and coronary heart disease. Meta-analysis of prospective studies. *Circulation* 102: 1082-1085.

48. Erqou, S., S. Kaptoge, P. L. Perry, E. Di Angelantonio, A. Thompson, I. R. White, S. M. Marcovina, R. Collins, S. G. Thompson, and J. Danesh. 2009. Lipoprotein(a) concentration and the risk of coronary heart disease, stroke, and nonvascular mortality. *JAMA* 302: 412-423.

49. Glader, C. A., L. S. Birgander, H. Stenlund, and G. H. Dahlén. 2002. Is lipoprotein(a) a predictor for survival in patients with established coronary artery disease? Results from a prospective patient cohort study in northern Sweden. *J. Intern. Med* 252: 27-35.

50. Zeljkovic, A., N. Bogavac-Stanojevic, Z. Jelic-Ivanovic, V. Spasojevic-Kalimanovska, J. Vekic, and S. Spasic. 2009. Combined effects of small apolipoprotein (a) isoforms and small, dense LDL on coronary artery disease risk. *Arch. Med. Res* 40: 29-35.

51. Cantin, B., F. Gagnon, S. Moorjani, J. P. Després, B. Lamarche, P. J. Lupien, and G. R. Dagenais. 1998. Is lipoprotein(a) an independent risk factor for ischemic heart disease in men? The Quebec Cardiovascular Study. *J. Am. Coll. Cardiol* 31: 519-525.

52. Kronenberg, F., M. F. Kronenberg, S. Kiechl, E. Trenkwalder, P. Santer, F. Oberhollenzer, G. Egger, G. Utermann, and J. Willeit. 1999. Role of lipoprotein(a) and apolipoprotein(a) phenotype in atherogenesis: prospective results from the Bruneck study. *Circulation* 100: 1154-1160.

53. Ariyo, A. A., C. Thach, and R. Tracy. 2003. Lp(a) lipoprotein, vascular disease, and mortality in the elderly. *N. Engl. J. Med* 349: 2108-2115.

54. Luc, G., J. Bard, D. Arveiler, J. Ferrieres, A. Evans, P. Amouyel, J. Fruchart, and P. Ducimetiere. 2002. Lipoprotein (a) as a predictor of coronary heart disease: the PRIME Study. *Atherosclerosis* 163: 377-384.

55. Suk Danik, J., N. Rifai, J. E. Buring, and P. M. Ridker. 2006. Lipoprotein(a), measured with an assay independent of apolipoprotein(a) isoform size, and risk of future cardiovascular events among initially healthy women. *JAMA* 296: 1363-1370.

56. Milionis, H. J. 2000. Lipoprotein (a) and Stroke. *J Clin Pathol.* 53: 487-496.

57. Rath, M., A. Niendorf, T. Reblin, M. Dietel, H. J. Krebber, and U. Beisiegel. 1989. Detection and quantification of lipoprotein(a) in the arterial wall of 107 coronary bypass patients. *Arteriosclerosis* 9: 579-592.

58. D'Angelo, A., D. Geroldi, M. A. Hancock, V. Valtulina, A. I. Cornaglia, C. A. Spencer, E. Emanuele, A. Calligaro, M. L. Koschinsky, P. Speziale, and L. Visai. 2005. The apolipoprotein(a) component of lipoprotein(a) mediates binding to laminin: contribution to selective retention of lipoprotein(a) in atherosclerotic lesions. *Biochim. Biophys. Acta* 1687: 1-10.

59. Edelstein, C., D. Pfaffinger, J. Hinman, E. Miller, G. Lipkind, S. Tsimikas, C. Bergmark, G. S. Getz, J. L. Witztum, and A. M. Scanu. 2003. Lysine-phosphatidylcholine adducts in kringle V impart unique immunological and potential pro-inflammatory properties to human apolipoprotein(a). *J. Biol. Chem* 278: 52841-52847.

60. Marcovina, S. M., and M. L. Koschinsky. 2003. Evaluation of lipoprotein(a) as a prothrombotic factor: progress from bench to bedside. *Curr. Opin. Lipidol* 14: 361-366.

61. Koschinsky, M. L. 2004. Lipoprotein(a) and the link between atherosclerosis and thrombosis. *Can J Cardiol* 20 Suppl B: 37B-43B.

62. Marcucci, R., A. A. Liotta, A. P. Cellai, A. Rogolino, A. M. Gori, B. Giusti, D. Poli, S. Fedi, R. Abbate, and D. Prisco. 2003. Increased plasma levels of lipoprotein(a) and the risk of idiopathic and recurrent venous thromboembolism. *Am. J. Med* 115: 601-605.

63. Nowak-Göttl, U., R. Sträter, A. Heinecke, R. Junker, H. G. Koch, G. Schuierer, and A. von Eckardstein. 1999. Lipoprotein (a) and genetic polymorphisms of clotting factor V, prothrombin, and methylenetetrahydrofolate reductase are risk factors of spontaneous ischemic stroke in childhood. *Blood* 94: 3678-3682.

64. Sträter, R., S. Becker, A. von Eckardstein, A. Heinecke, S. Gutsche, R. Junker, K. Kurnik, R. Schobess, and U. Nowak-Göttl. 2002. Prospective assessment of risk factors for recurrent stroke during childhood--a 5-year follow-up study. *Lancet* 360: 1540-1545.

65. Ignatescu, M., K. Kostner, G. Zorn, M. Kneussl, G. Maurer, I. M. Lang, and K. Huber. 1998. Plasma Lp(a) levels are increased in patients with chronic thromboembolic pulmonary hypertension. *Thromb. Haemost* 80: 231-232.

66. Edelberg, J. M., M. Gonzalez-Gronow, and S. V. Pizzo. 1990. Lipoprotein(a) inhibition of plasminogen activation by tissue-type plasminogen activator. *Thromb. Res* 57: 155-162.

67. Sangrar, W., L. Bajzar, M. E. Nesheim, and M. L. Koschinsky. 1995. Antifibrinolytic effect of recombinant apolipoprotein(a) in vitro is primarily due to attenuation of tPA-mediated Glu-plasminogen activation. *Biochemistry* 34: 5151-5157.

68. Loscalzo, J. 1990. Lipoprotein(a). A unique risk factor for atherothrombotic disease. *Arteriosclerosis* 10: 672-679.

69. Feric, N. T., M. B. Boffa, S. M. Johnston, and M. L. Koschinsky. 2008. Apolipoprotein(a) inhibits the conversion of Glu-plasminogen to Lys-plasminogen: a novel mechanism for lipoprotein(a)-mediated inhibition of plasminogen activation. *J. Thromb. Haemost* 6: 2113-2120.

70. Devlin, C. M., S. Lee, G. Kuriakose, C. Spencer, L. Becker, I. Grosskopf, C. Ko, L. Huang, M. L. Koschinsky, A. D. Cooper, and I. Tabas. 2005. An apolipoprotein(a) peptide delays chylomicron remnant clearance and increases plasma remnant lipoproteins and atherosclerosis in vivo. *Arterioscler. Thromb. Vasc. Biol* 25: 1704-1710.

71. Gazzaruso, C., D. Geroldi, A. Garzaniti, C. Falcone, P. Fratino, G. Finardi, and P. Buscaglia. 1998. Apolipoprotein(a) phenotypes as genetic markers of coronary atherosclerosis severity. *Int. J. Cardiol* 64: 277-284.

72. Ducas, J., C. Silversides, T. C. Dembinski, M. C. Y. Chan, R. Tate, A. Dick, P. Nixon, S. Ren, and G. X. Shen. 2002. Apolipoprotein(a) phenotypes predict the severity of coronary artery stenosis. *Clin Invest Med* 25: 74-82.

73. Gensini, G. G. 1975. Indications for cardiac catheterization, angiography, and coronary arteriography. *Geriatrics* 30: 63-68.

74. Kang, C., M. Dominguez, S. Loyau, T. Miyata, V. Durlach, and E. Anglés-Cano. 2002. Lp(a) particles mold fibrin-binding properties of apo(a) in size-dependent manner: a study with different-length recombinant apo(a), native Lp(a), and monoclonal antibody. *Arterioscler. Thromb. Vasc. Biol* 22: 1232-1238.

75. Emanuele, E., E. Peros, P. Minoretti, A. D'Angelo, L. Montagna, C. Falcone, and D. Geroldi. 2004. Significance of apolipoprotein(a) phenotypes in acute coronary syndromes: relation with clinical presentation. *Clin. Chim. Acta* 350: 159-165.

76. Rifai, N., J. Ma, F. M. Sacks, P. M. Ridker, W. J. L. Hernandez, M. J. Stampfer, and S. M. Marcovina. 2004. Apolipoprotein(a) size and lipoprotein(a) concentration and future risk of angina pectoris with evidence of severe coronary atherosclerosis in men: The Physicians' Health Study. *Clin. Chem* 50: 1364-1371.

77. Wild, S. H., S. P. Fortmann, and S. M. Marcovina. 1997. A prospective case-control study of lipoprotein(a) levels and apo(a) size and risk of coronary heart disease in Stanford Five-City Project participants. *Arterioscler. Thromb. Vasc. Biol* 17: 239-245.

78. Klausen, I. C., A. Sjøl, P. S. Hansen, L. U. Gerdes, L. Møller, L. Lemming, M. Schroll, and O. Faergeman. 1997. Apolipoprotein(a) isoforms and coronary heart disease in men: a nested case-control study. *Atherosclerosis* 132: 77-84.

79. Gambhir, J. K., H. Kaur, K. M. Prabhu, J. D. Morrisett, and D. S. Gambhir. 2008. Association between lipoprotein(a) levels, apo(a) isoforms and family history of premature CAD in young Asian Indians. *Clin. Biochem* 41: 453-458.

80. Dirisamer, A., H. Widhalm, E. Aldover-Macasaet, S. Molzer, and K. Widhalm. 2008. Elevated Lp(a) with a small apo(a) isoform in children: risk factor for the development of premature coronary artery disease. *Acta Paediatr* 97: 1653-1657.

81. Zorio, E., C. Falco, M. A. Arnau, F. España, A. Osa, L. A. Ramon, R. Castello, L. Almenar, M. A. Palencia, and A. Estelles. 2006. Lipoprotein (a) in young individuals as a marker of the presence of ischemic heart disease and the severity of coronary lesions. *Haematologica* 91: 562-565.

82. Dobson, C. M. 2003. Protein folding and misfolding. *Nature* 426: 884-890.

83. Kuznetsov, G., and S. K. Nigam. 1998. Folding of Secretory and Membrane Proteins. *N Engl J Med* 339: 1688-1695.

84. Wang, J., and A. L. White. 2000. Role of calnexin, calreticulin, and endoplasmic reticulum mannosidase I in apolipoprotein(a) intracellular targeting. *Biochemistry* 39: 8993-9000.

85. White, A. L., D. L. Rainwater, J. E. Hixson, L. E. Estlack, and R. E. Lanford. 1994. Intracellular processing of apo(a) in primary baboon hepatocytes. *Chem. Phys. Lipids* 67-68: 123-133.

86. Quinones, Q. J., G. G. de Ridder, and S. V. Pizzo. 2008. GRP78: a chaperone with diverse roles beyond the endoplasmic reticulum. *Histol. Histopathol* 23: 1409-1416.

87. Kleizen, B., and I. Braakman. 2004. Protein folding and quality control in the endoplasmic reticulum. *Curr. Opin. Cell Biol* 16: 343-349.

88. Brodsky, J. L. 2007. The protective and destructive roles played by molecular chaperones during ERAD (endoplasmic-reticulum-associated degradation). *Biochem. J* 404: 353-363.

89. McMillan, D. R., M. J. Gething, and J. Sambrook. 1994. The cellular response to unfolded proteins: intercompartmental signaling. *Curr. Opin. Biotechnol* 5: 540-545.

90. Ellgaard, L., and A. Helenius. 2003. Quality control in the endoplasmic reticulum. *Nat. Rev. Mol. Cell Biol* 4: 181-191.

91. Ellgaard, L., and E. Frickel. 2003. Calnexin, calreticulin, and ERp57: teammates in glycoprotein folding. *Cell Biochem. Biophys* 39: 223-247.

92. Danilczyk, U. G., M. F. Cohen-Doyle, and D. B. Williams. 2000. Functional relationship between calreticulin, calnexin, and the endoplasmic reticulum luminal domain of calnexin. *J. Biol. Chem* 275: 13089-13097.

93. Ellgaard, L., and A. Helenius. 2001. ER quality control: towards an understanding at the molecular level. *Curr. Opin. Cell Biol* 13: 431-437.

94. Ellgaard, L., R. Riek, D. Braun, T. Herrmann, A. Helenius, and K. Wüthrich. 2001. Three-dimensional structure topology of the calreticulin P-domain based on NMR assignment. *FEBS Lett* 488: 69-73.

95. Kopito, R. R. 1997. ER quality control: the cytoplasmic connection. *Cell* 88: 427-430.

96. Mast, S. W., K. Diekman, K. Karaveg, A. Davis, R. N. Sifers, and K. W. Moremen. 2005. Human EDEM2, a novel homolog of family 47 glycosidases, is involved in ER-associated degradation of glycoproteins. *Glycobiology* 15: 421-436.

97. Hosokawa, N., I. Wada, Y. Natsuka, and K. Nagata. 2006. EDEM accelerates ERAD by preventing aberrant dimer formation of misfolded alpha1-antitrypsin. *Genes Cells* 11: 465-476.

98. Appenzeller-Herzog, C., and L. Ellgaard. 2008. The human PDI family: versatility packed into a single fold. *Biochim. Biophys. Acta* 1783: 535-548.

99. Gillece, P., J. M. Luz, W. J. Lennarz, F. J. de La Cruz, and K. Römisch. 1999. Export of a cysteine-free misfolded secretory protein from the endoplasmic reticulum for degradation requires interaction with protein disulfide isomerase. *J. Cell Biol* 147: 1443-1456.

100. Frickel, E., R. Riek, I. Jelesarov, A. Helenius, K. Wuthrich, and L. Ellgaard. 2002. TROSY-NMR reveals interaction between ERp57 and the tip of the calreticulin P-domain. *Proc. Natl. Acad. Sci. U.S.A* 99: 1954-1959.

101. Leach, M. R., M. F. Cohen-Doyle, D. Y. Thomas, and D. B. Williams. 2002. Localization of the lectin, ERp57 binding, and polypeptide binding sites of calnexin and calreticulin. *J. Biol. Chem* 277: 29686-29697.

102. Ciechanover, A., A. Orian, and A. L. Schwartz. 2000. Ubiquitin-mediated proteolysis: biological regulation via destruction. *Bioessays* 22: 442-451.

103. Gabel, B., Z. Yao, R. S. McLeod, S. G. Young, and M. L. Koschinsky. 1994. Carboxyl-terminal truncation of apolipoproteinB-100 inhibits lipoprotein(a) particle formation. *FEBS Lett* 350: 77-81.

104. Lobentanz, E. M., K. Krasznai, A. Gruber, C. Brunner, H. J. Müller, J. Sattler, H. G. Kraft, G. Utermann, and H. Dieplinger. 1998. Intracellular metabolism of human apolipoprotein(a) in stably transfected Hep G2 cells. *Biochemistry* 37: 5417-5425.

105. Koschinsky, M. L., J. E. Tomlinson, T. F. Zioncheck, K. Schwartz, D. L. Eaton, and R. M. Lawn. 1991. Apolipoprotein(a): expression and characterization of a recombinant form of the protein in mammalian cells. *Biochemistry* 30: 5044-5051.

106. Wang, J., and A. L. White. 1999. Role of N-linked glycans, chaperone interactions and proteasomes in the intracellular targeting of apolipoprotein(a). *Biochem. Soc. Trans* 27: 453-458.

107. Schainfeld, R. M. 2001. Management of peripheral arterial disease and intermittent claudication. *J Am Board Fam Pract* 14: 443-450.

108. Sacco, R. L. 2001. Newer risk factors for stroke. *Neurology* 57: S31-34.

109. Cheng, S. W., A. C. Ting, and J. Wong. 1997. Lipoprotein (a) and its relationship to risk factors and severity of atherosclerotic peripheral vascular disease. *Eur J Vasc Endovasc Surg* 14: 17-23.

110. Peng, D. Q., S. P. Zhao, and J. L. Wang. 1999. Lipoprotein (a) and apolipoprotein E epsilon 4 as independent risk factors for ischemic stroke. *J Cardiovasc Risk* 6: 1-6.

111. Price, J. F., A. J. Lee, A. Rumley, G. D. Lowe, and F. G. Fowkes. 2001. Lipoprotein (a) and development of intermittent claudication and major cardiovascular events in men and women: the Edinburgh Artery Study. *Atherosclerosis* 157: 241-249.

112. LAEMMLI, U. K. 1970. Cleavage of Structural Proteins during the Assembly of the Head of Bacteriophage T4. *Nature* 227: 680-685.

113. White, A. L., D. L. Rainwater, and R. E. Lanford. 1993. Intracellular maturation of apolipoprotein[a] and assembly of lipoprotein[a] in primary baboon hepatocytes. *J. Lipid Res* 34: 509-517.

114. Dill, K. A., and H. S. Chan. 1997. From Levinthal to pathways to funnels. *Nat. Struct. Biol* 4: 10-19.

115. Sali, A., E. Shakhnovich, and M. Karplus. 1994. How does a protein fold? *Nature* 369: 248-251.

116. Lobentanz, E. M., and H. Dieplinger. 1997. Biogenesis of lipoprotein(a) in human and animal hepatocytes. *Electrophoresis* 18: 2677-2681.

117. Sylvester-Hvid, C., N. Kristensen, T. Blicher, H. Ferré, S. L. Lauemøller, X. A. Wolf, K. Lamberth, M. H. Nissen, L. Ø. Pedersen, and S. Buus. 2002. Establishment of a quantitative ELISA capable of determining peptide - MHC class I interaction. *Tissue Antigens* 59: 251-258.

118. Muresan, Z., and P. Arvan. 1997. Thyroglobulin transport along the secretory pathway. Investigation of the role of molecular chaperone, GRP94, in protein export from the endoplasmic reticulum. *J. Biol. Chem* 272: 26095-26102.

119. Cornell, R. 1989. Chemical cross-linking reveals a dimeric structure for CTP:phosphocholine cytidylyltransferase. *J. Biol. Chem* 264: 9077-9082.

120. Cardoso-Saldaña, G., A. De La Peña-Díaz, J. Zamora-González, R. Gomez-Ortega, C. Posadas-Romero, R. Izaguirre-Avila, E. Malvido-Miranda, M. E. Morales-Anduaga, and E. Anglés-Cano. 2006. Ethnicity and lipoprotein(a) polymorphism in Native Mexican populations. *Ann. Hum. Biol* 33: 202-212.